AUTHOR(S): IBIE, C., KNOTT, R. and THOMPSON, C.J.

TITLE: In-vitro evaluation of the effect of polymer structure on uptake of novel polymer-insulin polyelectrolyte complexes by human epithelial cells.

YEAR: 2015

Publisher citation: IBIE, C., KNOTT, R. and THOMPSON, C.J. 2015. In-vitro evaluation of the effect of polymer structure on uptake of novel polymer-insulin polyelectrolyte complexes by human epithelial cells. International journal of pharmaceutics [online], 479(1), pages 103-117. Available from: https://doi.org/10.1016/j.ijpharm.2014.12.058

OpenAIR citation: IBIE, C., KNOTT, R. and THOMPSON, C.J. 2015. In-vitro evaluation of the effect of polymer structure on uptake of novel polymer-insulin polyelectrolyte complexes by human epithelial cells. International journal of pharmaceutics, 479(1), pages 103-117. Held on OpenAIR [online]. Available from: https://openair.rgu.ac.uk

Available online 27 December 2014 – International Journal of Pharmaceutics

IN VITRO EVALUATION OF THE EFFECT OF POLYMER STRUCTURE ON UPTAKE OF NOVEL POLYMER-INSULIN POLYELECTROLYTE COMPLEXES BY HUMAN EPITHELIAL CELLS

IBIE C., KNOTT R. AND THOMPSON C.J.*

***CORRESPONDING AUTHOR: +441224 262561; C.THOMPSON@RGU.AC.UK**

INSTITUTE FOR HEATH AND WELLBEING RESEARCH, ROBERT GORDON UNIVERSITY, ABERDEEN, AB10 7GJ, UK.

ABSTRACT

The biocompatibility and cellular uptake of polymer, insulin polyelectrolyte complexes (PECs) prepared using polyallylamine-based polymers was evaluated *in-vitro* using Caco-2 cell monolayers as a predictive model for human small intestinal epithelial cells.

Poly(allyl amine) (PAA) and Quaternised PAA (QPAA) were thiolated using either carbodiimide mediated conjugation to *N*-acetylcysteine (NAC) or reaction with 2-iminothiolane hydrochloride yielding their NAC and 4-thiobutylamidine (TBA) conjugates, respectively.

The effect of polymer quaternisation and/or thiolation on the IC_{50} of PAA was determined by 3-(4,5-dimethylthiazol-2-yl)-2,5-diphenyltetrazolium bromide (MTT) assay carried out on Caco-2 cells (with and without a 24 h recovery period after samples were removed). Uptake of PECs by Caco-2 cells was monitored by microscopy using fluorescein isothiocyanate (FITC) labelled insulin and rhodamine-labelled polymers at polymer:insulin ratios (4:5) after 0.5, 1, 2 and 4 h incubation in growth media (± calcium) and following pre-incubation with insulin.

MTT results indicated that quaternisation of PAA was associated with an improvement in IC_{50} values; cells treated with QPAA (0.001-4 $mgmL^{-1}$) showed no signs of toxicity following a 24 h cell recovery period, while thiolation of QPAA resulted in a decrease in the IC_{50}.

Cellular uptake studies showed that within 2-4 h, QPAA and QPAA-TBA insulin PECs were taken up intracellularly, with PECs being localised within the perinuclear area of cells. Further investigation showed that uptake of PECs was unaffected when calcium-free media was used, while presaturating insulin receptors affected the uptake of QPAA, insulin PECs, but not QPAA-TBA PECs.

The biocompatibility of PAA and uptake of insulin was improved by both thiol and quaternary substitution.

KEYWORDS: Fluorescence microscopy; insulin; MTT assay; polyelectrolyte complex; thiolation; quaternization.

49 **1. INTRODUCTION**

50 Oral delivery of insulin, used for the management of type 1 diabetes, could be referred to as
51 one of the major long term goals of pharmaceutical research. Oral administration of insulin is,
52 however, currently not feasible and exogenous insulin formulations are often given
53 subcutaneously (Belchetz and Hammond, 2004). This is a constraint for the management of
54 diabetes as the chronic nature of the condition requires regular injections. It is known that the
55 regular injection regimen required for the management of diabetes predisposes diabetics to
56 physiological stress due to multiple daily injections and has associated risk of infections
57 and/or local reactions at injection sites as well as problems encountered during the insulin
58 administration process such as precipitation of insulin in the injection pump (Wong, 2010).
59 Parenteral administration of insulin also creates a significant difference in the normal
60 physiological distribution of insulin in the body (Chen et al., 2011 and Ehud Arbit and
61 Kidron, 2009) which may be associated with the occurrence of peripheral hyperinsulinaemia
62 and insulin resistance resulting in hypoglycaemia, weight gain, neuropathy, retinopathy,
63 atherosclerosis and hypertension in most diabetics (Ehud Arbit and Kidron, 2009).
64 Oral delivery of insulin has the potential to eliminate these problems and offers an excellent
65 alternative being the easiest and most convenient route of drug administration (Narayani,
66 2001). Physiological distribution of orally administered insulin also mimics the natural
67 physiological fate of insulin in the body, closely replicating the direct delivery of endogenous
68 insulin to the liver (Satake et al., 2002). Oral insulin delivery is, however, mitigated by the
69 susceptibility of insulin to proteolytic digestion in the gastrointestinal tract (GIT) as insulin is
70 degraded by pepsin in gastric juice and proteases (carboxypeptidase, α-chymotrypsin and
71 trypsin) in the intestinal lumen (Carino and Mathiowitz, 1999, Chen et al., 2011, Ehud Arbit
72 and Kidron, 2009 and Wong, 2010). Also, insulin a large, hydrophilic macromolecule with
73 logP value < 0 exhibits poor permeation through the GIT epithelium unaided either

74 trancellularly or paracellularly. The presence of a layer of mucus above the intestinal mucosa
75 also constitutes a further permeation barrier (Bendayan et al., 1994, Carino and Mathiowitz,
76 1999 and Morishita and Peppas, 2006).
77 Polyelectrolyte complexes (PECs) formed spontaneously by electrostatic interaction between
78 oppositely charged polyelectrolytes have been found to have potential applications for the
79 formulation of oral protein delivery systems. At physiologic pH, cationic polymers like
80 chitosan and polyallylamine which feature protonable amine groups can undergo electrostatic
81 complexation with negatively charged insulin forming PECs. These PECs are present in
82 aqueous or buffer solutions as positively charged, spherical nanoparticles, with hydrodynamic
83 sizes between 100-400 nm (Mao et al., 2005). Incorporating insulin intended for oral
84 administration into particles of this size has been shown to enhance transcytotic uptake of
85 insulin-loaded particles through Peyer's patches (Lee, 1988, Rao and Ritschel, 1995 and Shah
86 et al., 2002). The process of polyelectrolyte complexation also conveniently creates a
87 platform where various functionalities that enhance oral insulin bioavailability can be
88 imparted into the delivery system through rational modification of the carrier polymer
89 structure. Also, the presence of a positive charge on these complexes may provide additional
90 advantages like improved paracellular and transcellular transport of nanocomplexes as a
91 result of electrostatic interaction with anionic components of epithelial cell tight junctions
92 and cell membrane glycoproteins. Transmucosal transport is also facilitated by electrostatic
93 interaction of PECs with anionic sulphate residues and sialic acid present in the intestinal
94 mucosa (Lee, 1988, Rao and Ritschel, 1995 and Shah et al., 2002).
95 Polymer quaternisation which stabilises and maximises cationic charge may, therefore,
96 enhance processes like tight junction opening, insulin complexation and mucoadhesion that
97 benefit from charge-based interactions. Quaternisation also improves the biocompatibility of
98 polycationic polymers like PAA and polylysine which have been observed to be cytotoxic as

99 their free protonable amine groups have the ability to interact with anionic portions of
100 glycoproteins on the cell membrane causing apoptosis (Slita et al., 2007). Quaternisation
101 decreases the number of these protonable primary amine groups per molecule minimising
102 toxicity (Brownlie et al., 2004). Other polymer modification processes like thiolation are
103 directed at facilitating polymer-mucin interactions by introducing thiol-disulphide bonding
104 between polymer and mucus thereby improving mucoadhesion of the dosage form. Thiolation
105 has also been shown to reduce efflux of absorbed materials as well as limit some enzymatic
106 degradation of proteins due to the chelating effect thiol groups can have (Lee, 1988, Rao and
107 Ritschel, 1995 and Shah et al., 2002).
108 A series of polyallylamine-based amphiphillic polymers (AP) consisting of PAA modified
109 with hydrophobic pendant groups (palmitoyl, cetyl and cholesteryl groups) have been used
110 previously in the formulation of PECs for oral insulin delivery (Thompson et al., 2008,
111 Thompson et al., 2010 and Thompson et al., 2009). These AP were further modified by
112 quaternisation. Complexation with negatively charged insulin was carried out in pH 7.4 Tris
113 buffer resulting mostly in spherical nano-sized complexes. PECs prepared using palmitoyl
114 grafted PAA (Pa)/QPAA (QPa) exhibited the best insulin loading efficiency and protection
115 from peptic and tryptic degradation (Thompson et al., 2010 and Thompson et al., 2009).
116 Palmitoyl grafted PAA showed 2-3 fold increase in IC_{50} value compared to PAA. The nature
117 of the polymer used in PEC formulation was observed to play a vital role in determining the
118 cellular uptake of the resultant complexes. Major factors that were found to affect the ability
119 of the polymer to facilitate polymer-insulin PEC uptake include structural composition of the
120 polymer, charge density, polymer conformation as well as hydrophilic/lipophilic balance
121 (Fischer et al., 2003, Florence et al., 2000 and Malik et al., 2000).
122 This study aims to further develop this work by modifying PAA to include one of two distinct
123 thiol moieties (N-acetyl cysteine or 4-thiobutylamidine) as well as quaternary ammonium

124 moieties. The IC_{50} of these polymers against Caco-2 cells was ascertained using an MTT
125 assay. These novel polymers were then complexed with insulin over a range of
126 polymer:insulin ratios to ascertain their optimal mixing ratio by determination of
127 complexation efficiency (using HPLC), size and zeta potential (using photon correlation
128 spectroscopy) and %transmittance. Optimal ratio PECs were then used to treat a model gut
129 epithelial cell line (Caco-2) to determine the effect of polymer architecture on PEC and
130 polymer uptake (via fluorescence microscopy and fluorimetry, respectively).
131
132
133
134
135
136
137
138
139
140
141
142
143
144
145
146
147

2. MATERIALS AND METHODS

2.1. MATERIALS

Poly(allylamine hydrochloride) (average Mw = 15 kDa), tris(hydroxymethyl)aminomethane (Tris base) (≥ 99%), *N*-(3-Dimethylaminopropyl)-*N*'-ethyl carbodiimide hydrochloride (EDAC), sodium hydroxide, *N*-hydroxysuccinimide (NHS), *N*-acetylcysteine, 2-iminothiolane hydrochloride, sodium borohydride, iodine solution (0.5M), starch solution (2%), rhodamine B isothiocyanate (RBITC), fluorescein isothiocyanate (FITC)-insulin, Eagle's minimum essential medium (EMEM), calcium-free EMEM, 3-(4,5-dimethylthiazol-2-yl)-2,5-diphenyl tetrazolium bromide (MTT), Triton X-100, dimethylsulfoxide (DMSO) HPLC grade, Glycine, Dulbecco's phosphate buffered saline (PBS), sodium dodecyl sulphate (SDS) and trypan blue were from Sigma Aldrich, UK.

Caco-2 cells were obtained from ECACC, Wiltshire UK and were used passage number 45-70. L-glutamine (200 mM), non-essential amino acids, trypsin-EDTA (0.05 %) and DAPI were purchased from Invitrogen, Scotland. Foetal calf serum-activated (FCS) was obtained from Biosera, UK. All other reagents used were of analytical grade.

2.2. POLYMER SYNTHESIS AND CHARACTERISATION

2.2.1. Extraction of PAA base from hydrochloride and Quaternisation of PAA

The methods used for the purification of the free PAA base from PAA hydrochloride and subsequent quaternisation of PAA to yield QPAA have been previously described in earlier reports published by our group (Narayani and Panduruanga Rao, 1995). The degree of quaternisation of the product was estimated by elemental analysis; samples (1 mg) were

analysed using a Perkin Elmer series 2 elemental analyser (Perkin Elmer, UK) and results were obtained in triplicate.

2.2.2. Thiolation of PAA and QPAA

Thiolation of PAA and QPAA by conjugation to *N*-acetylcysteine via an amide bond was carried out using a similar method to Yin et al. (Yin et al., 2009). *N*-acetylcysteine (250 mg; 1.53 mmol) was dissolved in 100 ml of deionised water into which EDAC and NHS were added consecutively up to a final concentration of 200 mM each to activate the carboxylic acid groups of *N*-acetylcysteine. The mixture was adjusted to pH 4-5 using 2 M HCl and left stirring at room temperature for 1 h, after which PAA/QPAA (250 mg) was added into the reaction mixture and the pH of the mixture readjusted to between pH 4-5. The reaction was carried out under nitrogen at room temperature for 5 h without exposure to light. A control experiment containing equivalent concentrations of *N*-acetylcysteine and PAA without EDAC/NHS was also set up in the same way and allowed to run simultaneously.

The thiolation of PAA and QPAA using amidine linkages was carried out as described previously (Bernkop-Schnürch et al., 2003). Briefly, PAA/QPAA (500 mg) was dissolved in 50 ml deionised water and the pH adjusted to 6.5 using 5 M HCl. 2-iminothiolane hydrochloride (400 mg) was added into the flask, and the reaction left stirring under nitrogen. The experiment was conducted at room temperature in the dark for 14 h.

The reaction mixtures for the thiolation experiments were dialysed (molecular weight cut-off – 7 kDa) in the dark at 4 °C, once against 5 L of 5 mM HCl, twice against 5 L of 5 mM HCl containing 1 % NaCl, once again against 5 L of 5 M HCl and finally against 5 L of 0.4 mM HCl. The various polymer conjugates isolated by dialysis were then freeze dried over 48 h using a VirTis adVantage freeze drier (Biopharma Process Systems, UK), characterised and stored at -20 °C.

2.2.3. Determination of free thiol and disulphide content

The amount of free thiol groups immobilised on each thiolated conjugate was estimated by iodometric titration using a 1 % starch solution as an indicator. Each thiomer (10 mg) was dissolved in 1 ml of deionised water acidified with a drop of 2 M HCl. 1 % starch indicator (300 µl) was added into the polymer solution before titrating the solution with a 1 mM iodine solution until a permanent blue colour characteristic of the iodine-starch complex was observed (Vigl et al., 2009). The amount of thiol groups in mols per gram of polymer was estimated from a calibration plot prepared from titrating iodine against increasing concentrations (2-100 $mgml^{-1}$) of an *N*-acetylcysteine reference standard (n=3; R^2= 0.99). The total amount of thiol substituents (free and oxidised) immobilised on a gram of each polymer was obtained by reducing disulphide bonds (formed during thiolation) with sodium borohydride ($NaBH_4$) to free thiols. Briefly, a 1 ml solution (1 $mgml^{-1}$) of each thiomer in pH 7.4 Tris buffer was prepared in a glass vial and mixed with 4 % sodium borohydride solution (2 ml) and incubated at 37 °C for 1 h in a shaking water bath. The reaction was then stopped by slowly adding 400 µl of 5 M HCl with gentle stirring. Each reaction mixture obtained was immediately subjected to iodometric titration as described above to obtain free thiol content. The disulphide bond content of each thiomer was estimated by subtracting the free thiol content obtained for each polymer prior to the reduction process from the total thiol content which was obtained after treatment with the reducing agent. Experiments were carried out in triplicate.

2.2.4. Zeta potential

The zeta potential (mV) of 1 $mgml^{-1}$ polymer solutions in Tris buffer pH 7.4 contained in folded capillary cells was determined at 25°C by photon correlation spectroscopy (PCS) (Zetasizer Nano-ZS, Malvern Instruments, UK) (Thompson et al., 2009).

2.3. *IN-VITRO* POLYMER BIOCOMPATIBILITY TESTING

The IC_{50} value of each test polymer was determined by MTT assay (Mosmann, 1983). Caco-2 cells grown in supplemented EMEM (containing 10 % (v/v) FCS, 1 % (v/v) non-essential amino acids and 1 % (v/v) L-glutamine) at 37 °C, 5 % CO_2 and 95 % humidity were used to seed 96-well plates at a cell density of 10,000 cells/200 µl of cell suspension per well. The cells were grown for 72 h, after which the culture media was aspirated and replaced with 200 µl of polymer solutions (concentrations ranging between 0.001-0.5 $mgml^{-1}$) prepared in supplemented EMEM without FCS (to avoid interaction of polymers with FCS). Positive and negative control wells were prepared by treating cells with 200µl of EMEM (without FCS) and 1 % Triton-X (in PBS), respectively.

The plate was incubated for 24 h at 37 °C, 5 % CO_2 and 95 % humidity, after which 50 µl of MTT (5 $mgml^{-1}$ in PBS) was added into each well. The plate was subsequently wrapped in tin foil (to protect it from light) and incubated for 4 h. The plate contents were subsequently aspirated and each well was then filled with DMSO (200 µl) followed by 25 µl of glycine buffer (7.5 gL^{-1} glycine, 5.9 gL^{-1} NaCl, pH 10.5). The plate was analysed by UV spectrophotometry (SoftMax Pro 5.0, Molecular Devices, U.S.A.) at 570 nm and cell viability (%) was calculated relative to the negative (cells treated with Triton-X in PBS) and positive (untreated cells in EMEM) controls (Thompson et al., 2009). The MTT assay was repeated for each polymer using cells allowed a 24 h recovery period in fresh supplemented culture media (with FCS) post-treatment with polymer solutions. Plots of % cell viability against polymer concentration were used to determine the IC_{50} value of the different polymers with/without a recovery period.

2.4. CELLULAR UPTAKE STUDIES

2.4.1. Preparation of RBITC-labelled polymers and fluorescent polymer, insulin PECs

For non-thiolated polymers, PAA and QPAA, 5 ml of RBITC in DMSO (1 $mgml^{-1}$) was added dropwise over 10 min into 95 ml of a 0.05 % (w/v) solution of polymer in double-distilled water with gentle magnetic stirring. The stirring was continued for one h and the mixture dialysed (molecular weight cut-off – 7 kDa; Medicell UK) against 5 L of double-distilled water for 48 h with 6 water changes every 24 h (Lin et al., 2008).

For thiolated polymers, methanol was used instead of DMSO to dissolve RBITC and the pH of the reaction kept at pH 4-5 using 5 M HCl to limit oxidation of thiol groups to disulphides (Ma et al., 2008). The reaction was also carried out under nitrogen and the mixture dialysed in the dark (MW cutoff-7 kDa; Medicell UK) against 5 L of 5 mM HCl for 24 h and then 5 L of 0.4 mM HCl for a further 24 h (6 changes every 24 h).

The polymer solution obtained from the dialysis process was freeze dried over 48 h to yield a deep pink to purple solid.

RBITC-tagged polymers were used in preparing fluorescent polymer, insulin nanocomplexes by mixing RBITC-labelled polymer with FITC-insulin at polymer:insulin (P: I) mass ratios of 4:5 (0.2:0.25 $mgml^{-1}$) in Tris buffer pH 7.4. This mass ratio was arrived at by polymer-insulin complexation optimisation experiments based on complexation efficiency, hydrodynamic diameter and %Transmittance values observed over a 48 h time course (data not shown).

2.4.2. Monitoring cellular uptake of PECs by fluorescence microscopy

Caco-2 cells were seeded at a density of 1 X 10^5 $cellsml^{-1}$ in 24 well plates and grown over 3 days at 5 % CO_2, 95 % humidity and 37 °C (Thompson et al., 2011). The media contained in the wells was aspirated and washed with PBS. Fluorescent complexes were prepared in pH

7.4 Tris buffer by mixing RBITC-labelled polymer with FITC-insulin at mass ratios of 4:5 (0.2:0.25 $mgml^{-1}$). These complexes were then diluted in FCS-free media to obtain concentrations of 0.005:0063 and 0.016:0.020 $mgml^{-1}$ for non-quaternised and quaternised polymer complexes, respectively. The PEC concentrations used for the uptake experiments were based on the IC_{50} values of each polymer obtained from MTT assays conducted without a recovery period. Wells were treated with PECs and incubated for time periods of 0.5, 1, 2 or 4 h. PEC uptake experiments were also carried out after reducing the concentration of quaternised polymers used to that of non-quaternised polymers (0.005:0063 $mgml^{-1}$) to enable detection of concentration-based differences in uptake profile.

After incubation PECs were removed and the cell layer subsequently washed (x2) with PBS and stained with 18.8 μgml^{-1} solution of DAPI in PBS for 10 min to highlight the nuclear region of the cells (Tyrer et al., 2002). The wells were then washed (x2) with PBS and treated with trypan blue to highlight non-viable cells. Uptake of complexes was assessed by examining cells using a fluorescence microscope (Leica DMI4000B, Leica Microsystems Ltd. UK) (x20 objective lens). Images were captured on a camera fitted to the microscope and are indicative of replicate wells (n=3). Uptake of control, polymer only, solutions at the same concentrations and time intervals was also assessed by fluorescence microscopy.

2.4.3. Quantification of polymer uptake

Caco-2 cells were cultured and treated with RBITC-labelled polymers (PAA, QPAA, QPAA-NAC and QPAA-TBA) using concentrations equivalent to that used in earlier uptake experiments over 2 h. The cell layer was then washed (x 3) with PBS and the cell layer attached to each well treated with 1 ml of 2 % SDS in PBS solution for 30 min to lyse cells (Yin et al., 2009). The fluorescence intensity of the cell lysate obtained from the above procedure was measured by fluorescence spectrophotometer (Perkin Elmer LS55

Fluorescence Spectrophotometer, Perkin-Elmer, UK) using a 1 ml quartz cuvette and excitation/emission wavelength set at 547/590 nm for RBITC. The results obtained were input into calibration curves (n=3; R^2 = 0.99) prepared using dilutions of the tagged polymers in 2 % SDS (concentrations ranging from 0.3-10 μgml^{-1}). The values obtained were subsequently used to estimate the percentage of tagged polymer taken up by the Caco-2 cells.

2.4.4. Investigation of PEC uptake mechanism

Uptake experiments similar to that described in 2.4.2 were carried out after incubating cells in calcium-free EMEM (FCS-free) for 2 h prior to treatment with PECs to inhibit calcium-dependent uptake mechanisms. Separate uptake experiments were also carried out using cell monolayers pre-incubated with 3 μgml^{-1} of free insulin for 1 h prior to polymer treatment to inhibit insulin-receptor mediated uptake mechanisms. Cell layers from these experiments were visualised under the fluorescence microscope and the results compared with that obtained from previous uptake experiments detailed in section 2.4.2. (Thompson et al., 2011)

2.5. STATISTICAL ANALYSIS

One-way ANOVA was used to analyse the effect of the respective polymers on cell viability using Tamhane T2 post-hoc test. The level of significance is represented as $p<0.05$ *: $p<;0.01$ ** or $p<0.001$ ***.

3.

3. RESULTS AND DISCUSSION

3.1. POLYMER SYNTHESIS AND CHARACTERISATION

After lyophilisation, all polymer conjugates appeared as white powders of fibrous structure which were readily soluble in aqueous media.

The average degree of quaternisation of QPAA as estimated by elemental analysis was found to be 72 ± 2 mol% (mean ± S.D; n=3) at an average yield of 76.2 ± 5% (mean ± S.D; n=3).

The percentage yield (mean ± S.D; n=3) of PAA-NAC, QPAA-NAC, PAA-TBA and QPAA-TBA conjugates was found to be 68.8 ± 2.8 %, 73.6 ± 2.3 %, 73.1 ± 4.4 % and 83.6 ± 7.7 %, respectively.

Immobilisation of reactive thiol groups on primary amino groups on the PAA/QPAA backbone was carried out using two types of covalent bonds. PAA and QPAA were coupled via a stable amide bond to *N*-acetylcysteine using a water-soluble carbodiimide cross-linker (EDAC) and NHS to form PAA/QPAA-*N*-acetylcysteine conjugates as shown in figure 1.

PAA and QPAA were also coupled to 4-thiobutylamidine via a reaction with 2-iminothiolane hydrochloride, a thiol-containing imidoester forming PAA/QPAA-4-thiobutylamidine conjugates. These TBA conjugates have a protonated amidine bond which bears an extra positive charge on the thiol constituent at pH 7.4 (Albrecht K, Bernkop-Schnürch, 2007 and Bacalocostantis et al., 2012) as can be seen in figure 2.

Optimisation of the coupling reaction between the polymers and *N*-acetylcysteine necessitated the inclusion of NHS in the cross-linking reaction to stabilise the *O*-acylisourea intermediate product of the EDAC-carboxylic acid reaction which is susceptible to hydrolysis and consequently has a short life span in aqueous media (Damink et al., 1996). The reaction was also carried out under nitrogen and at pH 4.5 to minimise oxidation of thiol groups to the reactive thiolate anion resulting in the formation of intramolecular disulphide bond formation

(Bernkop-Schnürch et al., 2004). An *N*-acylated amino acid was used during the reaction to prevent the occurrence of unwanted side reactions resulting in the formation of oligo/poly cysteine conjugates (Vigl et al., 2009). The zeta potential, total sulphydryl group content of each conjugate as well as the amount available as free thiols (SH) and disulphide (S-S) bonds are shown in table 1.

A negligible amount of thiol groups (0.2 ± 0.06 $\mu mol g^{-1}$ polymer) were detected in control samples obtained from similar NAC conjugation experiments carried out without the addition of EDAC/NHS. Results shown in table 1 indicate that the surface charge of the polymers varied with the nature of the substituting group. Quaternisation enhanced the cationic charge of PAA. Thiolation using 2-iminothiolane resulted in further increases of cationic charge of both parent polymers (PAA and QPAA) while conjugation of PAA/QPAA to NAC resulted in a reduction of cationic surface charge. This difference is probably related to the substitution of protonable primary amine groups with the uncharged amide bond present in NAC-based thiomers while the cationic substructure of the amidine group (figures 1 and 2) facilitates the retention of cationic charge in TBA-based thiomers. The marked variation in the surface charge of the thiomers obtained could have significant implications on the capacity of the polymer to complex with insulin as well as its ability to promote processes like tight junction opening and mucoadhesion that benefit from charge-based interactions. Polymer surface charge could also influence the biodistribution and cellular uptake of insulin PECs formed from the polymers (He et al., 2010 and Kotzé et al., 1997).

3.2. BIOCOMPATIBILITY TESTING

The toxicity profile of polymers was initially evaluated without the inclusion of a cell recovery period. Results from MTT assays conducted without a recovery period (WOR) were expressed as plots of % cell viability versus log polymer concentrations shown in figure 3.

371 IC_{50} values of each polymer obtained from MTT assays conducted without a recovery period
372 are highlighted in table 2.
373 The unmodified PAA backbone showed the highest toxicity having the lowest IC_{50} value of
374 0.009 ± 0.003 $mgml^{-1}$. This is expected as polycationic polymers like PAA and polylysine
375 have been observed to be cytotoxic due to the availability of free protonable amine groups
376 which have the ability to interact with anionic portions of glycoproteins on the cell membrane
377 causing apoptosis (Slita et al., 2007). Quaternisation decreases the number of these
378 protonable primary amine groups per molecule improving biocompatibility (Brownlie et al.,
379 2004), as may be seen by the marked improvement in IC_{50} exhibited by QPAA when
380 compared to the non-quaternised PAA backbone (tables 2 and 3). This is consistent with the
381 results obtained from other research groups where quaternisation of other polycations was
382 observed to be associated with improvements in their toxicity profile (Bernkop-Schnürch et
383 al., 2003).
384 Thiol substitution of the PAA backbone was also observed to result in an increase in IC_{50}
385 values (smaller than was obtained with quaternisation) with PAA-NAC displaying a lower
386 IC_{50} value than PAA-TBA (tables 2 and 3). This could be as a result of the lower level of
387 primary amine substitution found in PAA-NAC (total thiol substitution-340 ± 4.1 μmol
388 compared to 1080 ± 28 μmol thiol groups found in PAA-TBA) implying that PAA-NAC has
389 a higher level of free protonable primary amine groups to exert cytotoxic effects.
390 Thiolation of QPAA resulted in a reduction of IC_{50} suggesting that the thiol moieties had a
391 negative effect on biocompatibility of the quaternised PAA backbone. Thiols are capable of
392 covalent interactions (thiol-disulphide reactions) with glycoproteins and can consequently
393 damage protein components of cells irreversibly altering their structure/conformation (Wang
394 et al., 2004). Quaternisation increased the IC_{50} of PAA-NAC, but had no noticeable effect on
395 the IC_{50} of PAA-TBA. QPAA-TBA had the highest level of total substitution (thiol and

396 quaternary substitution combined) of primary amine groups and was therefore expected to
397 have the highest IC_{50} of all polymers tested. It was therefore surprising that PAA-TBA and
398 QPAA-TBA have approximately the same IC_{50} (0.02 $mgml^{-1}$) (tables 2 and 3). This implies
399 that the reduction in cytotoxic effects mediated by the quaternary groups present in QPAA-
400 TBA appear to have been completely mitigated by TBA-based thiol substitution, thereby
401 suggesting that the TBA thiol moiety may have toxic effects on cells. This also highlights the
402 fact that while quaternisation tends to completely mask the highly charged primary amine
403 groups of PAA limiting their ability to damage cells, thiolation may only result in the
404 replacement of one type of reactive groups (in this case free primary amine groups) with
405 another type (thiol groups). The cationic substructure of the amidine linkage also makes it
406 possible for these thiomers to initiate toxic effects associated with cationic charge as well as
407 effects arising from the actual thiol group as mentioned earlier, making these TBA conjugates
408 more toxic than their NAC-counterparts (Dwivedi et al., 2011).
409 The IC_{50} of each polymer was also evaluated after allowing the cells a 24 h recovery period in
410 supplemented EMEM post-treatment with polymers and similar plots of % cell viability
411 versus log polymer concentrations prepared (figure 4). The IC_{50} values of each polymer
412 obtained from MTT assays conducted with a recovery period are displayed in table 2. The
413 concentration at which a significant ($p<0.05$) drop in cell viability for each polymer are
414 displayed in table 3.
415 The purpose of introducing a recovery period was to determine the extent to which cells
416 could recover from the effect of the different polymers. This may give more insight on
417 whether the effect of the polymers on cells are transient/reversible (cytostatic) or permanent
418 (cytotoxic). Results shown in table 2 indicate that the inclusion of a recovery period before
419 treating the cells with MTT resulted in an increase in IC_{50} for all the polymers tested (figure

420 5). Indeed all polymers demonstrated a significant ($p<0.05$) increase in cell viability with a
421 recovery period (table 4).
422 QPAA appeared to only show a cytostatic effect as no loss of cell viability was observed (100
423 % cell viability) between the cencentration 0.001-4 $mgml^{-1}$ post-recovery. All other polymers
424 displayed reduced cell viability and thus cytotoxicity, but at higher concentrations than
425 without a recovery period.
426 NAC-based thiomers demonstrated a marked improvement (approximately 6-fold) in their
427 IC_{50} value after being subjected to a recovery period (figures 4 and 5). The effects of these
428 polymers on cells appear to have been cytostatic rather than cytotoxic at polymer low
429 concentrations, as cells were still viable and able to recover on removal of polymer solutions
430 and their replacement with fresh growth media. Hence this suggests that the effects of these
431 polymers on cells at low concentrations are largely reversible, and do not result in permanent,
432 irreparable damage.
433 On the other hand, polymers PAA and PAA-TBA showed little improvements in their IC_{50}
434 (about 1.5 fold) with the introduction of a recovery period (figure 5). This indicates that these
435 polymers have some cytotoxic properties, and their interactions with cells mostly causes
436 irreparable damage to cells and marked loss in cell viability. This again confirms the highly
437 cytotoxic effect of the primary amine groups in PAA and suggests the amidine thiol
438 substructure of PAA-TBA is a relatively cytotoxic moiety although less toxic than primary
439 amine groups (TBA substitution of PAA improved IC_{50} both with and/or without a recovery
440 period as may be seen in table 2 and 3). Bearing in mind that the difference in level of thiol
441 substitution between PAA-TBA and PAA-NAC may not allow direct comparison of their
442 toxic effects on cells, the presence of a protonable group within the amidine bond as
443 compared to the uncharged amide bonds of PAA-NAC (refer to figures 1 and 2) could
444 however result in an increase in potential to cause toxic effects. QPAA-TBA also appeared to

show cytostatic effects, although IC_{50} values were lower than QPAA and QPAA-NAC. The IC_{50} of QPAA-TBA was improved considerably after the introduction of a recovery period much higher than what was observed with PAA and PAA-TBA, but to a lesser extent to QPAA and QPAA-NAC.

Considering the results of the cytotoxicity assays conducted with and/or without a recovery period the toxicity profile of the parent polymer was found to play a role in determining the biocompatibility of the thiolated derivatives. For non-quaternised thiomers where the parent backbone PAA was cytotoxic, the toxicity profile of the polymers followed this order: PAA > PAA-TBA > PAA-NAC. While for quaternised polymers where the parent backbone QPAA was found to be less-cytotoxic , the toxicity profile of the thiomers followed this order QPAA-TBA > QPAA-NAC > QPAA. This may then indicate that when developing PAA-based thiomers, using QPAA as the parent polymer rather than PAA improves the biocompatibility of the resultant thiomers.

Futher biocompatibility issues to be aware of include the fact that the particulate nature of PEC delivery system may increase their potential to elicit immune responses *in-vivo* and affect its biodistribution/cellular trafficking altering their toxicity profile (Dufes et al., 2004 and Dwivedi et al., 2011). These however are factors to be considered in future work.

3.3. CELLULAR UPTAKE STUDIES

3.3.1. Fluorescence microscopy of polymer, insulin PECs

After a 2 h incubation of cells with fluorescent complexes, their uptake into Caco-2 cells was visualised using separate fluorescent filters (specific for insulin-FITC and RBITC-tagged polymers) and a FITC/RBITC combination filter to identify areas of polymer, insulin

469 colocalisation. Results are shown in figure 6 and are representative of images taken from one
470 of the replicate wells.

471 Only complexes prepared using QPAA and QPAA-TBA appear to be internalised by cells
472 (Figure 6). Polymer, insulin colocalisation was confirmed by the appearance of numerous
473 light yellow fluorescent spots within the cell layer as may be seen in figure 6A and 6B,
474 viewed using the RBITC/FITC combination filter. Cellular uptake of other complexes, e.g.
475 PAA, appeared to be more cell membrane-associated as fluorescence was observed mostly
476 round the cell membrane area (figure 6D).

477 Images were also taken of the same region of the cell layer using the different filter sets. The
478 brightfield image of the cell layer was also imaged after washing with trypan blue to
479 determine cell viability; the appearance of the blue/black trypan blue stain indicated non-
480 viable cells (figure 7A) were present. Very few cells were stained by trypan blue after 2 h
481 incubation with QPAA and QPAA-TBA (figures 7 and 8). This would suggest that the uptake
482 of PECs was not due to cell damage and was due to other uptake mechanisms.

483 The uptake process of QPAA and QPAA-TBA, insulin PECs was observed to be time-
484 dependent with the cell layer being observed to attain visible intracellular fluorescence (PEC
485 uptake) between 1-4 h (data not shown). The uptake process was also not affected by PEC
486 concentration as reducing PEC concentration to 0.005:0063 $mgml^{-1}$ (polymer:insulin) did not
487 inhibit the uptake of complexes (data not shown). The effect of increasing the amount of
488 PAA and non-quaternised complexes used (to match that used for quaternised polymers)
489 could not be evaluated because of the low IC_{50} of non-quaternised polymers.

490 In order to try and confirm the presence of PECs within the cells, the nuclei of Caco-2 cells
491 were stained with DAPI. For both QPAA and QPAA-TBA complex formulations, distinct
492 regions of PEC colocalisation with the blue DAPI stain could be observed (as bright spots),
493 suggesting that these complexes were located within the cell cytoplasm (figure 9). While

PAA complexes did not appear to be localised under the blue DAPI stain as can be seen in figure 9A.

The structure of the polymer used in PEC formulation was observed to play a role in determining the cellular uptake profile of different PECs by Caco-2 cells. Factors that may affect the ability of the polymer in facilitating PEC uptake include structural composition of the polymer, charge density, molecular weight, polymer conformation as well as hydrophilic/lipophilic balance (Fischer et al., 2003, Florence et al., 2000 and Malik et al., 2000).

3.3.2. Fluorescence microscopy and quantification of polymer uptake

Cellular uptake of RBITC-tagged polymer solutions (same concentrations as used for each PEC formulation) was also carried out by fluorescence microscopy (figures 10 and 11). While most quaternised polymers were taken up by cells, non-quaternised polymers were poorly taken up by Caco-2 cells with the exception of PAA. Quaternisation enhanced the uptake profile of PAA-NAC and PAA-TBA, confirming the importance of the quaternary group in promoting cellular uptake. Unlike their PEC formulations, PAA and QPAA-NAC were also taken up by Caco-2 cells as a shown in figures 10A and 11C. This implies that the properties of the original polymer may also be altered after complexation with insulin, resulting in a complex with different physicochemical properties from the parent molecules. Complexation of PAA and QPAA-NAC with insulin may have limited the ability of charged sites on these polymers to interact with the cell membrane and initiate uptake of PECs. This may be due to polymer, insulin complexation rendering charged sites on these polymers unavailable for interaction with the cell membrane. The PEC network may also create a steric barrier that prevents sites on the polymer from accessing compatible cell membrane components thereby limiting uptake (Harris and Chess, 2003). PAA and QPAA-NAC

polymers however show better uptake than PAA-TBA and PAA-NAC polymers as shown in figures 10 and 11.

Uptake of RBITC-tagged polymers was also quantified by fluorimetry after solubilising treated cell layers with 2 % SDS. This experiment was carried out for PAA, QPAA and thiolated QPAA. Thiolated PAA solutions were not analysed as their cellular uptake was observed to be poor. The results are detailed in table 5.

The results of the quantification experiment shown in table 5 are consistent with the results of fluorescence microscopy, showing that all quaternised polymers were taken up by the cells and the percentage of quaternised polymers taken up approximately double the amount of PAA uptake. The analysis was however not done with polymer, insulin complexes due to difficulties in obtaining a reliable calibration curve for insulin-FITC with the fluorimeter. (Fluorescence microscopy has shown polymer, insulin colocalisation was evident for QPAA and QPAA-TBA.) The results of the quantification process also confirm the fluorescence microscopy results which show cellular uptake of PAA and QPAA-NAC from their polymer solutions, even though uptake of their insulin PECs appeared to be negligible.

3.3.3. Identifying mechanisms of cellular uptake of PECs

To clarify the mechanisms involved in the cellular uptake of QPAA and QPAA-TBA PECs into the cytoplasm, Caco-2 cell layers were pre-incubated for 2 hs in calcium-free EMEM, to deplete cells of intracellular calcium stores, or incubated with free insulin (3 μgml^{-1}) for 1 h (to saturate insulin receptors) prior to treatment with QPAA, insulin and QPAA-TBA, insulin complexes. Cell layers were subsequently examined by fluorescence microscopy to observe any changes in the uptake profile of the aforementioned complexes (figures 12, 13, 14 and 15).

Figures 12 and 13 show the uptake of QPAA and QPAA-TBA, insulin PECs in calcium-free media compared to those from normal uptake conditions (FCS-free supplemented EMEM). Cells incubated in calcium-free media before treatment with QPAA and QPAA-TBA, insulin PECs were observed to show uptake similar to the results obtained in normal media, suggesting that the processes involved in the cellular uptake of both QPAA and QPAA-TBA insulin PECs appear independent of calcium-based mechanisms.

Pre-saturation of insulin receptors did not affect uptake of QPAA-TBA insulin complexes, which were still observed to be taken up regardless of the down-regulation of insulin receptors as shown in figure 14.

The pre-saturation process appeared to have a noticeable effect on the uptake of QPAA, insulin complexes as figure 15 shows that unlike figure 15A where the interior of the cells contains fluorescent spots figure 15B shows that uptake of QPAA complexes was affected by pre-saturating cell insulin receptors. The images taken with the RBITC and FITC filters also confirm poor uptake of the formulation (figures 15D and 15F, respectively). This suggests that uptake of QPAA, insulin complexes appears to benefit from interaction of complexed insulin with receptors on the cells and may also imply that the conformation of QPAA allows for complexed insulin to be held on or near the surface of the PEC enabling the insulin molecule adequate interaction with its receptor. Insulin receptors have been found to be present on the luminal surface of the small intestine (Buts et al., 1997) and several studies have confirmed active transcytosis of insulin through the intestinal epithelial cells (Bendayan et al., 1994 and King and Johnson, 1985). This highlights the active role the insulin receptor may play in the uptake of complexed insulin into the cells. Some reviews have however stated that for interaction of insulin with its receptor to take place, insulin has to be in its monomeric state and that insulin hexamer and aggregate formation is promoted by changes in environmental pH *in-vivo* (Russell-Jones, 2011). Hence complexation of insulin with QPAA

568 which possesses a quaternary group may limit pH-dependent changes of insulin from the
569 monomeric to the hexameric state enhancing insulin receptor–mediated uptake. The
570 stabilising effect of polymer-insulin linkage on insulin structure has been previously
571 documented by other groups. Linkage of Vit B_{12} or PEG to the Lys-29 residue of insulin was
572 reported to inhibit formation of the insulin hexamer, facilitating interaction of the insulin
573 monomer with insulin receptors on the surface of the epithelial cells and contributing to a
574 marked increase in the oral insulin bioavailability of these formulations (Petrus et al., 2002
575 and Still, 2002).
576 Further work is needed to clarify the exact mechanisms responsible for cellular uptake of
577 these complexes. This may involve the use of specific inhibitors like sodium azide which
578 inhibits metabolic processes as well as cytochalasin D and nocodazole, which are inhibitors
579 of the endocytotic trafficking pathway (Thompson et al., 2011). Hypothesizing on the fate of
580 the complexes in the cytosol, it is hoped that insulin PEC delivery systems will not only
581 initiate uptake of the protein, but also facilitate transport of complexes across the cells
582 (transcytosis). In an attempt to effect and control PEC uptake and transport in biological
583 systems, future work may be directed at functionalization of PECs using receptor-
584 recognisable ligands to facilitate active receptor-mediated transcytosis as opposed to relying
585 on passive uptake mechanisms depicted in the present work. This concept is already being
586 investigated by groups using the vit B_{12} ligand to produce receptor-mediated transcytosis of
587 nanoparticles via the vit B_{12} receptors (Chalasani et al., 2007).
588
589
590
591
592

4. CONCLUSION

The biocompatibility of the parent polymer PAA was improved by both thiol and quaternary substitution, with quaternisation offering a more substantial improvement in biocompatibility profile than thiolation. Thiolation was observed to lower the IC_{50} of QPAA, although QPAA, PAA-NAC and QPAA-NAC appeared to be largely cytostatic rather than cytotoxic. Uptake of polymer, insulin complexes by Caco-2 cells was observed to be highly dependent on polymer structure, with QPAA and QPAA-TBA showing the best potential for facilitating intracellular uptake of complexed insulin. Uptake of QPAA-TBA insulin PECs was found to be unaffected by down-regulation of insulin receptors and inhibition of calcium-dependent mechanisms, while cellular uptake of QPAA, insulin PECs was independent of calcium-based mechanisms but affected by down-regulation of insulin receptors. The results obtained indicate that these PAA-based polymer, insulin PECs specifically QPAA and QPAA-TBA formulations show considerable potential in promoting the delivery of insulin through the oral route.

ACKNOWLEDGEMENTS

The authors acknowledge the Institute for Health and Wellbeing Research, Robert Gordon University and the Scottish Overseas Research Scholarship Awards Scheme for providing the funding for this work.

REFERENCES

K. Albrecht , A. Bernkop-Schnürch. Thiomers: forms, functions and applications to nanomedicine. Nanomedicine, 2(1) (2007), pp. 41-50.

I. Bacalocostantis, V.P. Mane, M.S. Kang, A.S. Goodley, S. Muro, P. Kofinas. Effect of thiol pendant conjugates on plasmid DNA binding, release and stability of polymeric delivery vectors. Biomacromolecules, 13 (2012), pp. 1331-1339.

A. Bernkop-Schnürch, M. Hornof, T. Zoidl. Thiolated polymers-thiomers: synthesis and in vitro evaluation of chitosan-2-iminothiolane conjugates. International Journal of Pharmaceutics, 260(2) (2003), pp. 229-237.

A. Bernkop-Schnürch, A.H. Krauland, K. Leitner, T. Palmberger. Thiomers: potential excipients for non-invasive peptide delivery systems. European Journal of Pharmaceutics and Biopharmaceutics, 58 (2004), pp. 253-263.

P. Belchetz, P. Hammond, editors. Mosby's Color Atlas and Text of Diabetes and Endocrinology. Spain: Elselvier, 2004.

M. Bendayan, E. Ziv, D. Gingras, R. Ben-Sasson, H. Bar-on, M. Kidron. Biochemical and morpho-cytochemical evidence for the intestinal absorption of insulin in control and diabetic rats. Comparison between the effectiveness of duodenal and colon mucosa. Diabetologia, 37 (1994), pp. 119-126.

A. Brownlie, I.F. Uchegbu, A.G. Schatzlein. PEI based vesicle-polymer hybrid gene delivery system with improved biocompatibility. International Journal of Pharmaceutics, 274 (2004), pp. 41-52.

J.P. Buts, N. De Keyser, S. Marandi, A.S. Maernoudt, E.M. Sokal, J. Rahier, D. Hermans. Expression of insulin receptors and of 60-kDa receptor substrate in rat mature and immature enterocytes. American Journal of Physiology, Gastrointestinal and Liver Physiology, 273 (1997), pp. G217-G226.

641 G.P. Carino, E. Mathiowitz. Oral insulin delivery. Advanced Drug Delivery Reviews 35
642 (1999), pp. 249-257.

643 K.B. Chalasani, G.J. Russell-Jones, K.J. Akhlesh, P.V. Diwan, K.S. Jain. Effective oral
644 delivery of insulin in animal models using vitamin B12-coated dextran nanoparticles. Journal
645 of Controlled Release, 122 (2007), pp. 141-150.

646 M.C. Chen, K. Sonaje, K.J. Chen, H.W. Sung. A review of the prospects for polymeric
647 nanoparticle platforms in oral insulin delivery. Biomaterials, 32(36) (2011), pp. 9826-9838.

648 L.H.H.O. Damink, P.J. Dijkstra, M.J.A. Vanluyn, P.B. Vanwachem, P. Nieuwenhuis, J.
649 Feijen. Cross-linking of dermal sheep collagen using a water soluble carbodiimide.
650 Biomaterials, 17 (1996), pp. 765-773.

651 C. Dufes, I.F. Uchegbu, A.G. Schatzlein. Dendrimers in drug and gene delivery. In: I.F.
652 Uchegbu, A.G. Schatzlein, editors. Polymers in drug delivery. Taylor and Francis: Boca
653 Raton, 2004. pp. 199-235.

654 P.D. Dwivedi, A. Tripathi, K.M. Ansari, R. Shanker, M. Das. Impact of nanoparticles on the
655 immune system. Journal of Biomedical Nanotechnology, 7(1) (2011), pp. 193-194.

656 M.D. Ehud Arbit, M. Kidron. Oral insulin: The rationale for this approach and current
657 developments. Journal of Diabetes Science and Technology, 3(3) (2009), pp. 562-567.

658 D. Fischer, Y.X. Li, B. Ahlemeyer, J. Krieglstein, T. Kissel. In vitro cytotoxicity testing of
659 polycations: influence of polymer structure on cell viability and haemolysis. Biomaterials, 24
660 (2003), pp. 1121–1131.

661 A.T. Florence, T. Sakhivel, I. Toth. Oral uptake and translocation of a polylysine dendrimer
662 with a lipid surface. Journal of Controlled Release, 65(1-2) (2000), pp. 253-259.

663 J.M. Harris, R.B. Chess. Effect of pegylation on pharmaceuticals. Nature Review Drug
664 Discovery, 2(3) (2003), pp. 214-221.

C. He, Y. Hu, L. Yin, C. Tang, C. Yin. Effects of particle size and surface charge on cellular uptake and biodistribution of polymeric nanoparticles. Biomaterials, 31 (2010), pp. 3657-3666.

G.L. King, S. Johnson. Processing and transport of insulin by vascular endothelial cells. Effects of sulfonylureas on insulin receptors. Science, 227 (1985), pp. 183-1586.

A.F. Kotzé, H.L. Leußen, B.J. de Leeuw, B.G. de Boer, J.C. Verhoef, H.E. Junginger. *N*-Trimethyl chitosan chloride as a potential absorption enhancer across mucosal surfaces: in-vitro evaluation in intestinal epithelial cells (Caco-2). Pharmaceutical Research, 14(9) (1997), pp. 1197-1202.

V.H.L. Lee. Enzymatic barriers to peptide and protein absorption. Critical Review of Therapeutic Drug Carrier Systems, 5 (1988), pp. 69-97.

A. Lin, Y. Liu, Y. Huang, J. Sun, Z. Wu, X. Zhang, Q. Ping. Glycyrrhizin surface-modified chitosan nanoparticles for hepatocyte-targeted delivery. International Journal of Pharmaceutics 359 (1-2) (2008), pp. 247–53.

O. Ma, M. Lavertu, J. Sun, S. Nguyen, F.M. Buschmann, M.F. Winnik, C.D. Hoemann. Precise derivatization of structurally distinct chitosans with rhodamine B isothiocyanate. Carbohydrate Polymers, 72 (2008), pp. 616–624.

N. Malik, R. Wiwattanapatapee, R. Klopsch, K. Lorenz, H. Frey, J.W. Weener, E.W. Meijer, W. Paulus, R. Duncan. Dendrimers: relationship between structure and biocompatibility in vitro, and preliminary studies on the biodistribution of ^{125}I-labelled polyamidoamine dendrimers *in vivo*. Journal of Controlled Release, 65(1-2) (2000), pp. 133-148.

S. Mao, O. Germershaus, D. Fischer, T. Linn, R. Schnepf, T. Kissel. Uptake and transport of PEG-graft-trimethyl-chitosan copolymer-insulin nanocomplexes by epithelial cells. Pharmaceutical Research, 22 (2005), pp. 2058-2068.

689 M. Morishita, A.N. Peppas. Is the oral route possible for peptide and protein drug delivery?
690 Drug Discovery Today, 11 (2006), pp. 905-910.

691 T. Mosmann. Rapid colorimetric assay for cellular growth and survival: application to
692 proliferation and cytotoxicity assays. Journal of Immunological Methods, 65(1–2) (1983), pp.
693 55–63.

694 R. Narayani. Oral delivery of insulin-making needles needless. Trends in Biomaterials and
695 Artificial Organs, 15(1) (2001), pp. 12-16.

696 R. Narayani, K. Panduruanga Rao. Hypoglycemic effect of gelatin microspheres with
697 entrapped insulin and protease inhibitor in normal and diabetic rats. Drug Delivery, 2 (1995),
698 pp. 29-38.

699 A.K. Petrus, T.J. Fairchild, R.P. Doyle. Traveling the Vit B_{12} pathway: oral delivery of
700 protein and peptide drugs. Angew Chem Int Ed Engl, 48 (2002), pp. 1022-1028.

701 S. Rao, W.A. Ritschel. Colonic delivery of small peptides. STP Pharma Sciences, 5 (1995),
702 pp. 19-29.

703 G. Russell-Jones. Intestinal receptor targeting for peptide delivery: an expert's personal
704 perspective on reasons for failure and new opportunities. Therapeutic Delivery, 2(12) (2011),
705 pp. 1575-1593.

706 S. Satake, M.C. Moore, K. Igawa, M. Converse, B. Farmer, D.W. Neal, A.D. Cherrington.
707 Direct and indirect effects of insulin on glucose uptake and storage by the liver. Diabetes,
708 51(6) (2002), pp. 1663-1671.

709 R.B. Shah, F. Ahsan, M.A. Khan. Oral delivery of proteins: Progress and prognostication.
710 Critical Review of Therapeutic Drug Carrier Systems, 19 (2002), pp. 135-169.

711 A.V. Slita, N.A. Kasyanenko, O.V. Nazarova, I.I. Gavrilova, E.M. Eropkina, A.K. Sirotkin,
712 T.D. Smirnova, O.I. Kiselev, E.F. Panarin. DNA-polycation complexes: effect of polycation

713 structure on physic-chemical and biological properties. Journal of Biotechnology, 127 (2007),
714 pp. 679-693.

715 J.G. Still. Development of oral insulin: progress and current status. Diabetes Metabolism
716 Research and Reviews, 18(1) (2002), pp. 29-37.

717 C.J. Thompson, C. Ding, X. Qu, Z. Yang, I.F. Uchegbu, L. Tetley, W.P. Cheng. The effect of
718 polymer architecture on the nano self-assemblies based on novel comb-shaped amphiphillic
719 poly(allylamine). Colloid and Polymer Science, 286 (2008), pp. 1511-1526.

720 C.J. Thompson, P. Gadad, K. Skene, M. Smith, G. Smith, A. Mckinnon, W.P. Cheng, R.
721 Knott. Uptake and transport of novel amphiphillic polyelectrolyte-insulin nanocomplexes by
722 Caco-2 cells-towards oral insulin delivery. Pharmaceutical Research, 28 (2011), pp. 886-896.

723 C.J. Thompson, L. Tetley, W.P. Cheng. The influence of polymer architecture on the
724 protective effect of novel comb-shaped amphiphillic poly(allylamine) against in vitro
725 enzymatic degradation of insulin – Towards oral insulin delivery. International Journal of
726 Pharmaceutics, 260 (2010), pp. 229-237.

727 C.J. Thompson, L. Tetley, I.F. Uchegbu, W.P. Cheng. The complex between novel comb
728 shaped amphiphillic polyallyamine and insulin – Towards oral insulin delivery. International
729 Journal of Pharmaceutics, 376 (2009), pp. 216-227.

730 P. Tyrer, R. Foxwell, J. Kyd, M. Harvey, P. Sizer, A. Cripps. Validation and quantitation of
731 an in vitro M-cell model. Biochemical and Biophysical Research Communications, 299
732 (2002), pp. 377–383.

733 C. Vigl, K. Leitner, K. Albrecht, A. Bernkop-Schnürch. The efflux pump inhibitory
734 properties of (thiolated) polyallylamines. Journal of Drug Delivery Science and Technology,
735 19(6) (2009), pp. 405-411.

736 J. Wang, S.J. Gao, P.C. Zhang, S. Wang, H.Q. Mao, K.W. Leong. Polyphosphoramide gene
737 carriers: effect of charge group on gene transfer efficiency. Gene Therapeutics, 11 (2004), pp.
738 1001-1010.
739 W.T. Wong. Design of oral insulin delivery systems. Journal of Drug Targeting, 18(2)
740 (2010), pp. 79-92.
741 L. Yin, J. Ding, C. He, L. Cui, C. Tang, C. Yin. Drug permeability and mucoadhesion
742 properties of thiolated trimethyl chitosan nanoparticles in oral insulin delivery. Biomaterials,
743 30 (2009), pp. 5691-5700.
744
745
746
747
748
749
750
751
752
753
754
755
756
757
758
759

Legends to Figures

Fig. 1: Presumptive structure of repeating units of NAC conjugates of a) PAA: PAA-NAC b) QPAA:QPAA-NAC.

Fig. 2: Presumptive structure of repeating units of thiobutylamidine conjugates of a) PAA: PAA-TBA b) QPAA:QPAA-TBA.

Fig. 3: Caco-2 cell viability (%) as determined by MTT assay after 24 h exposure to varied concentrations of PAA, QPAA and their thiolated derivatives without a recovery period (n =3; ± S.D.).

Fig. 4: Caco-2 cell viability (%) as determined by MTT assay post-24 h recovery period and 24 h exposure to varied concentrations of PAA, QPAA and thiolated derivatives (n =3; ± S.D.).

Fig. 5: IC_{50} ($mgml^{-1}$) of polymers as determined by MTT assay without a recovery period (WOR) and post-24 h recovery period (WR) (n =3; ± S.D.). Key: WOR-without recovery period; WR – with recovery period.

Fig. 6: Fluorescent microscopy images of Caco-2 cells treated with A) QPAA, insulin PECs B) QPAA-TBA, insulin PECs C) QPAA-NAC, insulin PECs D) PAA, insulin PECs E) PAA-TBA, insulin PECs F) PAA-NAC, insulin PECs viewed using RBITC/FITC combination filter. Scale bar-50 µm.

Fig. 7: Fluorescent microscopy images of Caco-2 cells treated with QPAA, insulin complexes viewed using A) brightfield B) RBITC/FITC combination filter C) FITC filter D) RBITC filter. Scale bar-50 µm.

Fig. 8: Fluorescent microscopy images of Caco-2 cells treated with QPAA-TBA, insulin complexes viewed using A) brightfield B) RBITC/FITC combination filter C) FITC filter D) RBITC filter. Scale bar-50 μm.

Fig. 9: Fluorescent microscopy images of Caco-2 cells treated with PECs and DAPI. A) PAA PECs on RBITC/FITC combination filter B) QPAA PECs on RBITC/FITC combination filter C) QPAA-TBA PECs on RBITC/FITC combination filter. Scale bar-50 μm.

Fig. 10: Fluorescent microscopy images of Caco-2 cells treated with A) PAA C) PAA-TBA D) PAA-NAC; viewed using the RBITC filter. Scale bar-50 μm.

Fig. 11: Fluorescent microscopy images of Caco-2 cells treated with A) QPAA C) QPAA-TBA D) QPAA-NAC viewed using the RBITC filter. Scale bar-50 μm.

Fig. 12: Fluorescent microscopy images of Caco-2 cells post treatment with QPAA, insulin complexes in A) normal media-RBITC/FITC combination filter B) calcium-free media-RBITC/FITC combination filter C) normal media-RBITC filter D) calcium free media-RBITC filter E) normal media-FITC filter F) calcium free media-FITC filter. Scale bar-50 μm.

Fig. 13: Fluorescent microscopy images of Caco-2 cells post treatment with QPAA-TBA, insulin complexes in A) normal media-RBITC/FITC combination filter B) calcium-free media-RBITC/FITC combination filter C) normal media-RBITC filter D) calcium free media-RBITC filter E) normal media-FITC filter F) calcium free media-FITC filter. Scale bar-50 μm.

Fig. 14: Fluorescent microscopy images of Caco-2 cells treated with QPAA-TBA, insulin complexes where cell insulin receptors are A) normal-RBITC/FITC combination filter B) pre-saturated with insulin-RBITC/FITC combination filter C) normal-RBITC filter D) pre-

804 saturated with insulin-RBITC combination filter E) normal-FITC filter F) pre-saturated with
805 insulin-FITC combination filter. Scale bar-50 μm.

806 **Fig. 15**: Fluorescent microscopy images of Caco-2 cells treated with QPAA, insulin
807 complexes where cell insulin receptors are A) normal-RBITC/FITC combination filter B)
808 pre-saturated with insulin-RBITC/FITC combination filter C) normal-RBITC filter D) pre-
809 saturated with insulin-RBITC combination filter E) normal-FITC filter F) pre-saturated with
810 insulin-FITC combination filter. Scale bar-50 μm.

811

812

813

814

815

816

817

818

819

820

821

822

823

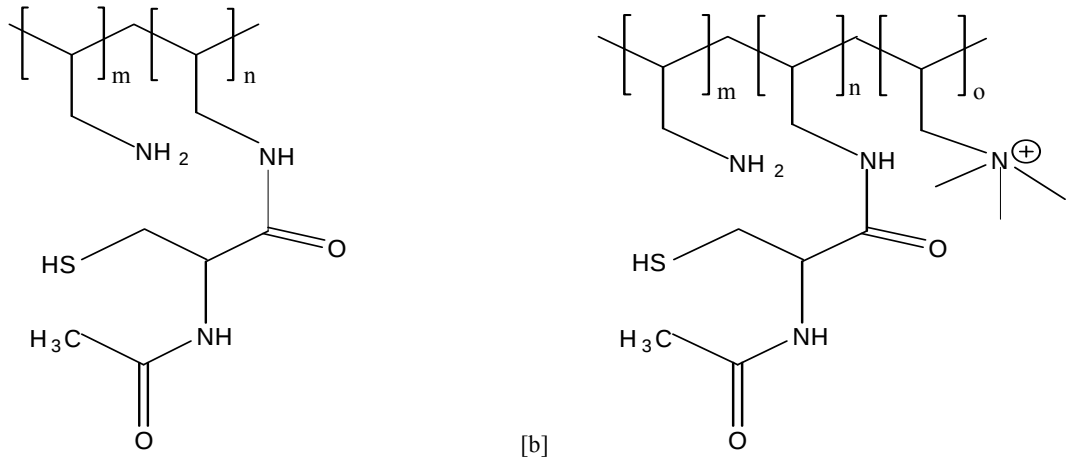

Fig. 1: Presumptive structure of repeating units of NAC conjugates of a) PAA: PAA-NAC b) QPAA:QPAA-NAC.

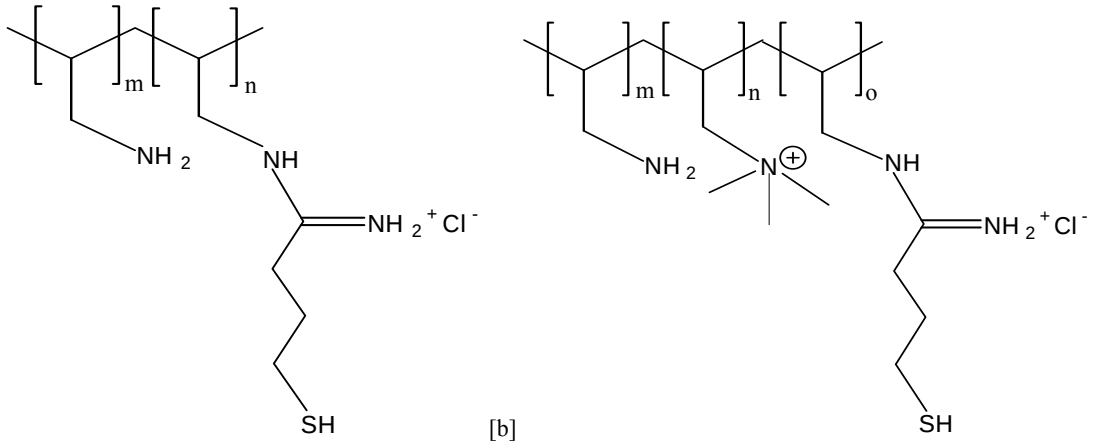

Fig. 2: Presumptive structure of repeating units of thiobutylamidine conjugates of a) PAA: PAA-TBA b) QPAA:QPAA-TBA.

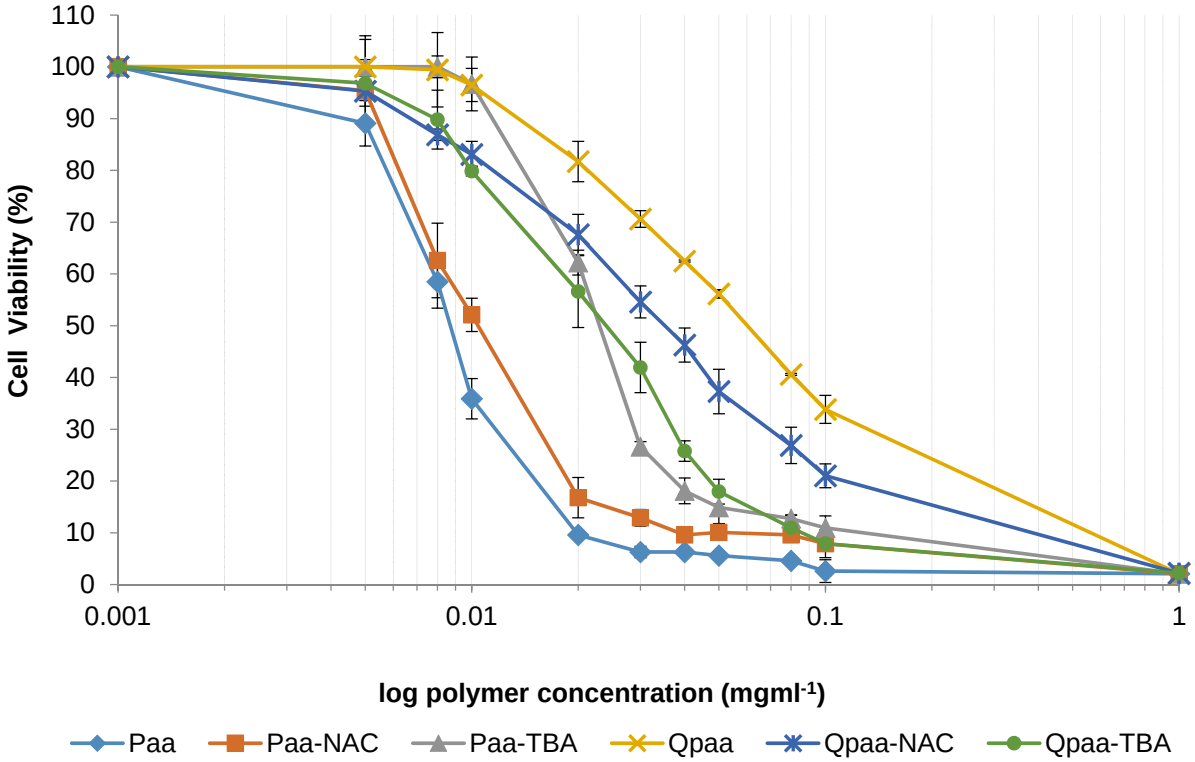

Fig. 3: Caco-2 cell viability (%) as determined by MTT assay after 24 h exposure to varied concentrations of PAA, QPAA and their thiolated derivatives without a recovery period (n=3; ± S.D.).

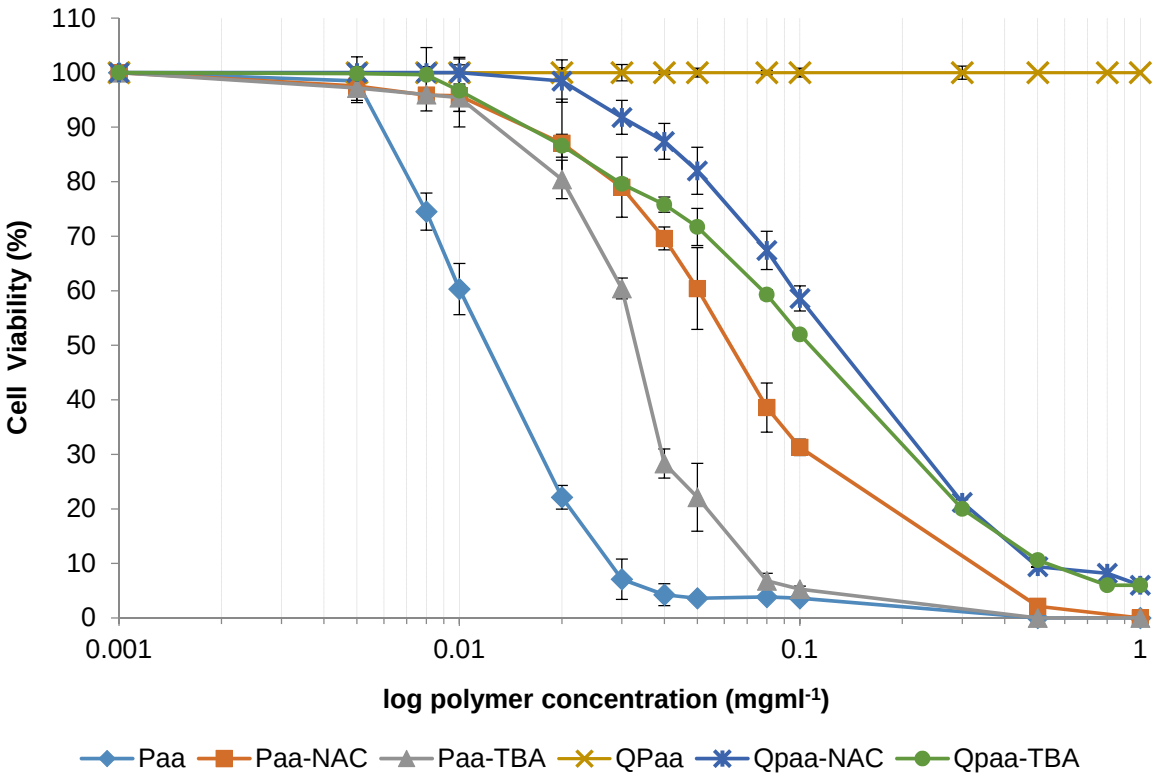

Fig. 4: Caco-2 cell viability (%) as determined by MTT assay post-24 h recovery period and 24 h exposure to varied concentrations of PAA, QPAA and thiolated derivatives (n=3; ± S.D.).

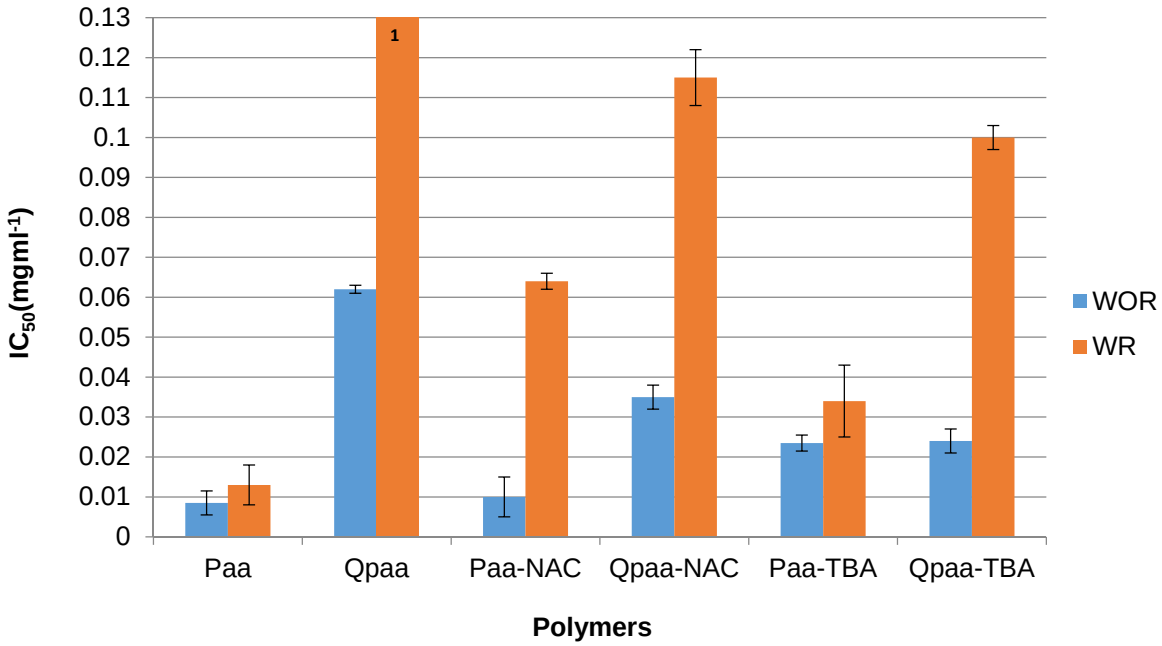

[1]Results obtained from the MTT assay of QPAA with a recovery period indicated that the IC_{50} of the polymer was higher than the highest polymer concentration tested (4 $mgml^{-1}$).

Fig. 5: IC_{50} ($mgml^{-1}$) of polymers as determined by MTT assay without a recovery period (WOR) and post-24 h recovery period (WR) (n =3; ± S.D.). Key: WOR-without recovery period; WR – with recovery period.

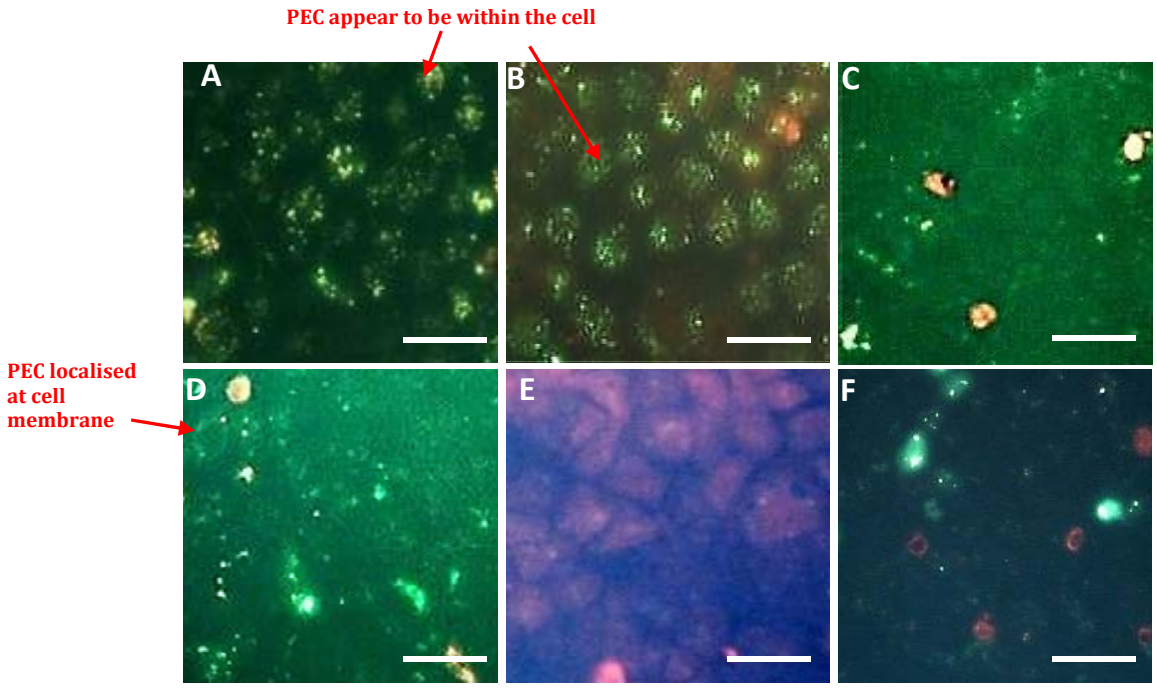

Fig. 6: Fluorescent microscopy images of Caco-2 cells treated with A) QPAA, insulin PECS B) QPAA-TBA, insulin PECS C) QPAA-NAC, insulin PECS D) PAA, insulin PECS E) PAA-TBA, insulin PECS F) PAA-NAC, insulin PECS viewed using RBITC/FITC combination filter. Scale bar-50 µm.

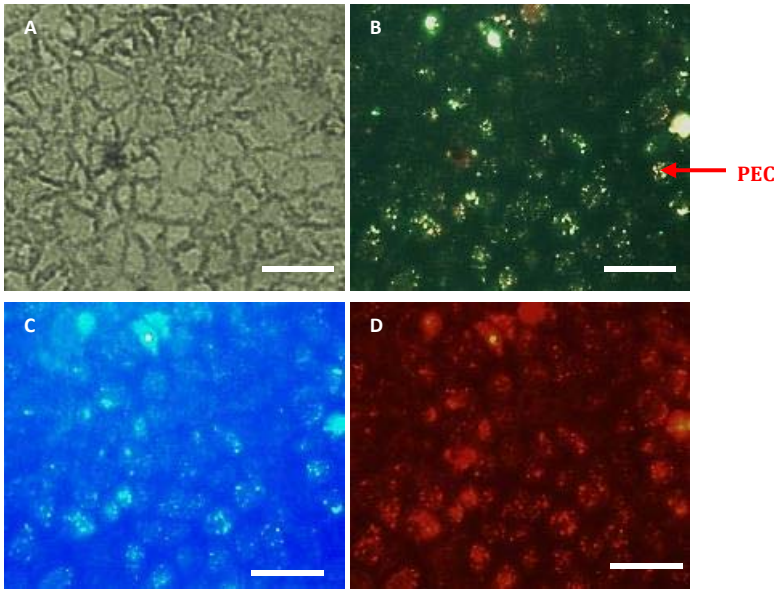

850

851 **Fig. 7**: Fluorescent microscopy images of Caco-2 cells treated with QPAA, insulin complexes viewed using A) brightfield

852 B) RBITC/FITC combination filter C) FITC filter D) RBITC filter. Scale bar-50 µm.

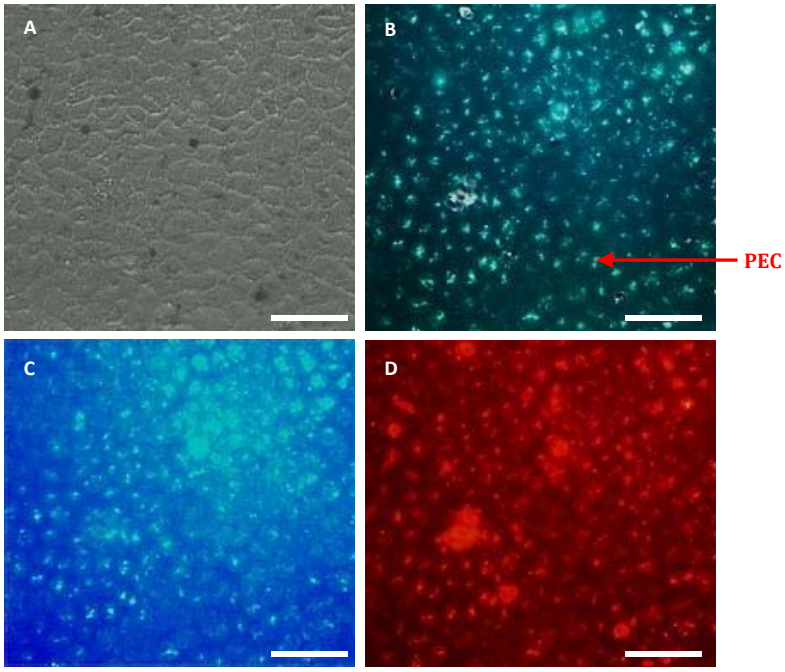

853

854 **Fig. 8**: Fluorescent microscopy images of Caco-2 cells treated with QPAA-TBA, insulin complexes viewed using A)

855 brightfield B) RBITC/FITC combination filter C) FITC filter D) RBITC filter. Scale bar-50 µm.

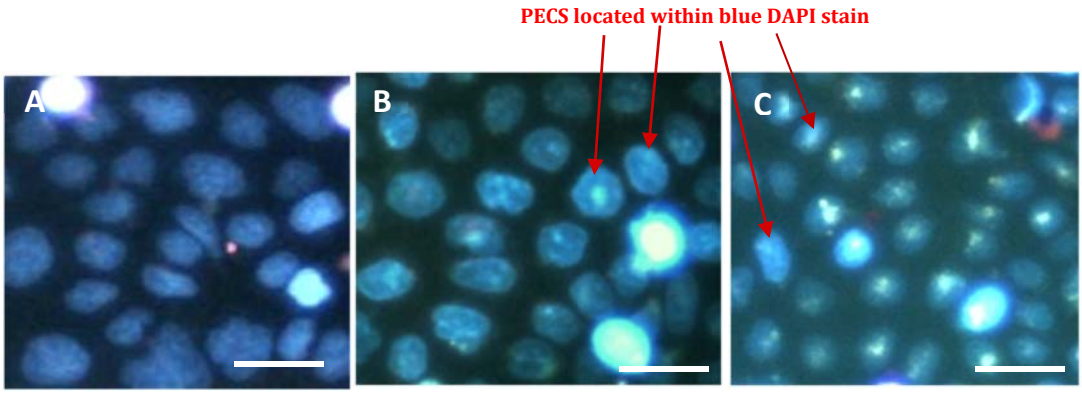

856

857 **Fig. 9**: Fluorescent microscopy images of Caco-2 cells treated with PECS and DAPI. A) PAA PECS on RBITC/FITC
858 combination filter B) QPAA PECS on RBITC/FITC combination filter C) QPAA-TBA PECS on RBITC/FITC combination
859 filter. Scale bar-50 µm.

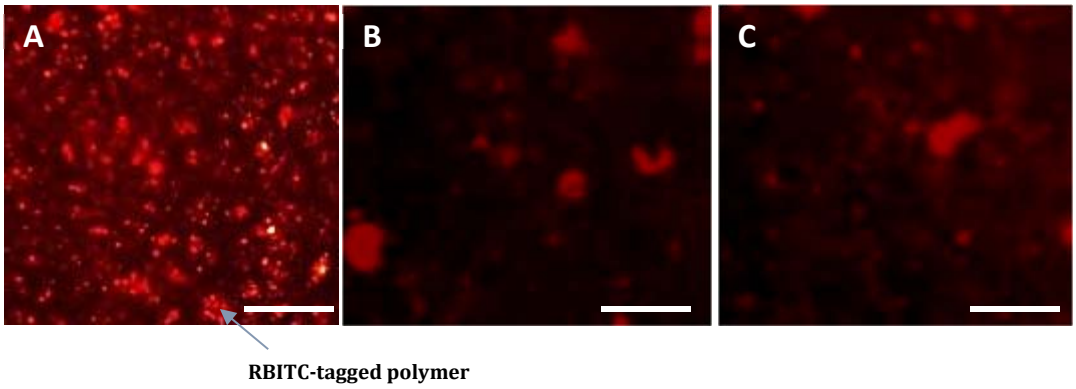

860

861 **Fig. 10**: Fluorescent microscopy images of Caco-2 cells treated with A) PAA C) PAA-TBA D) PAA-NAC; viewed using the
862 RBITC filter. Scale bar-50 µm.

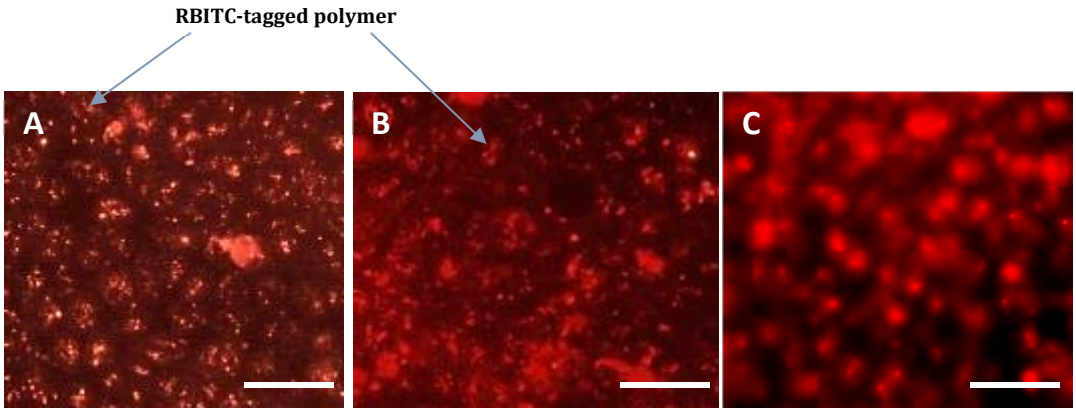

863

864 **Fig. 11**: Fluorescent microscopy images of Caco-2 cells treated with A) QPAA C) QPAA-TBA D) QPAA-NAC viewed
865 using the RBITC filter. Scale bar-50 µm.

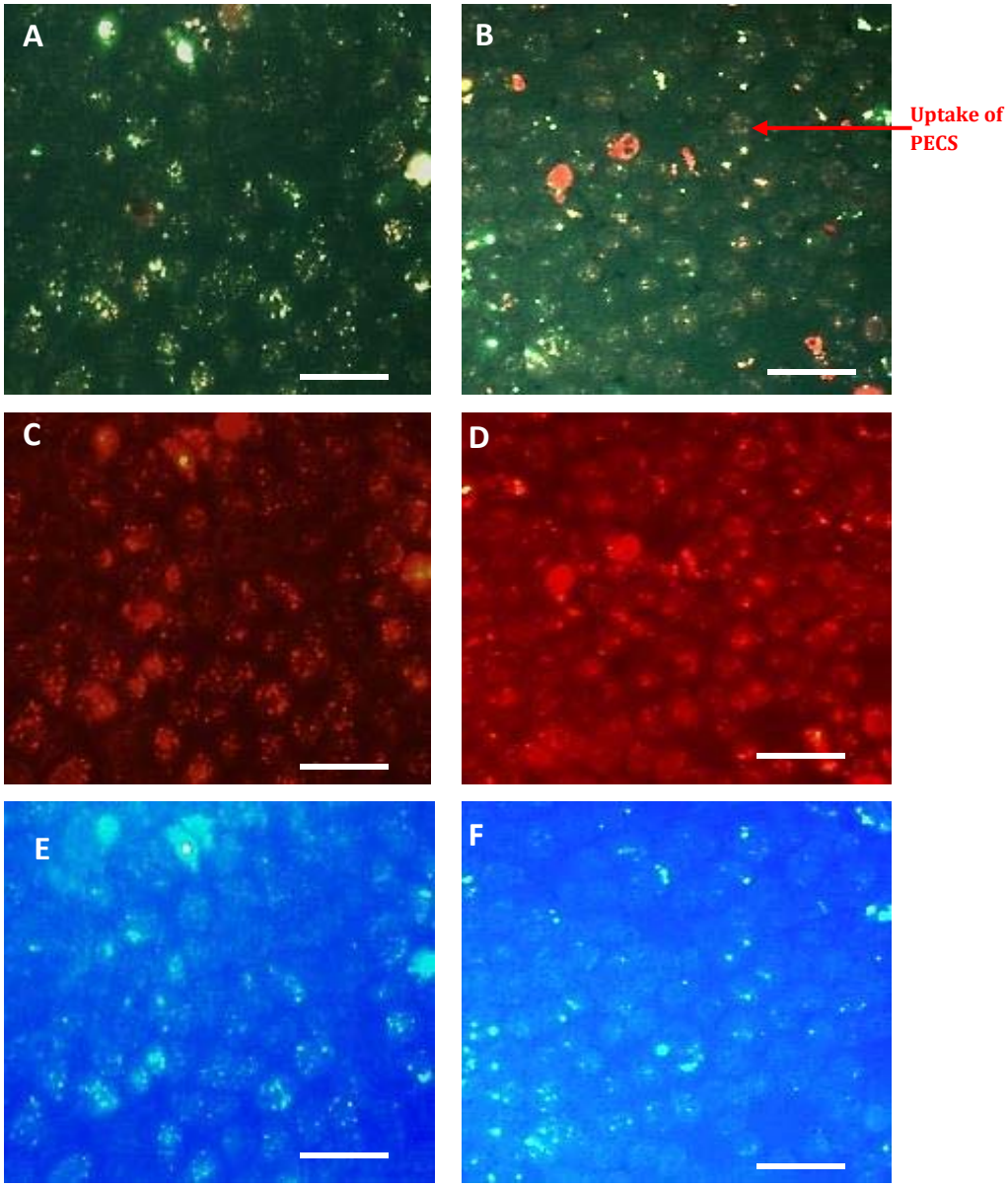

866

867 **Fig. 12**: Fluorescent microscopy images of Caco-2 cells post treatment with QPAA, insulin complexes in A) normal media-
868 RBITC/FITC combination filter B) calcium-free media-RBITC/FITC combination filter C) normal media-RBITC filter D)
869 calcium free media-RBITC filter E) normal media-FITC filter F) calcium free media-FITC filter. Scale bar-50 µm.

870

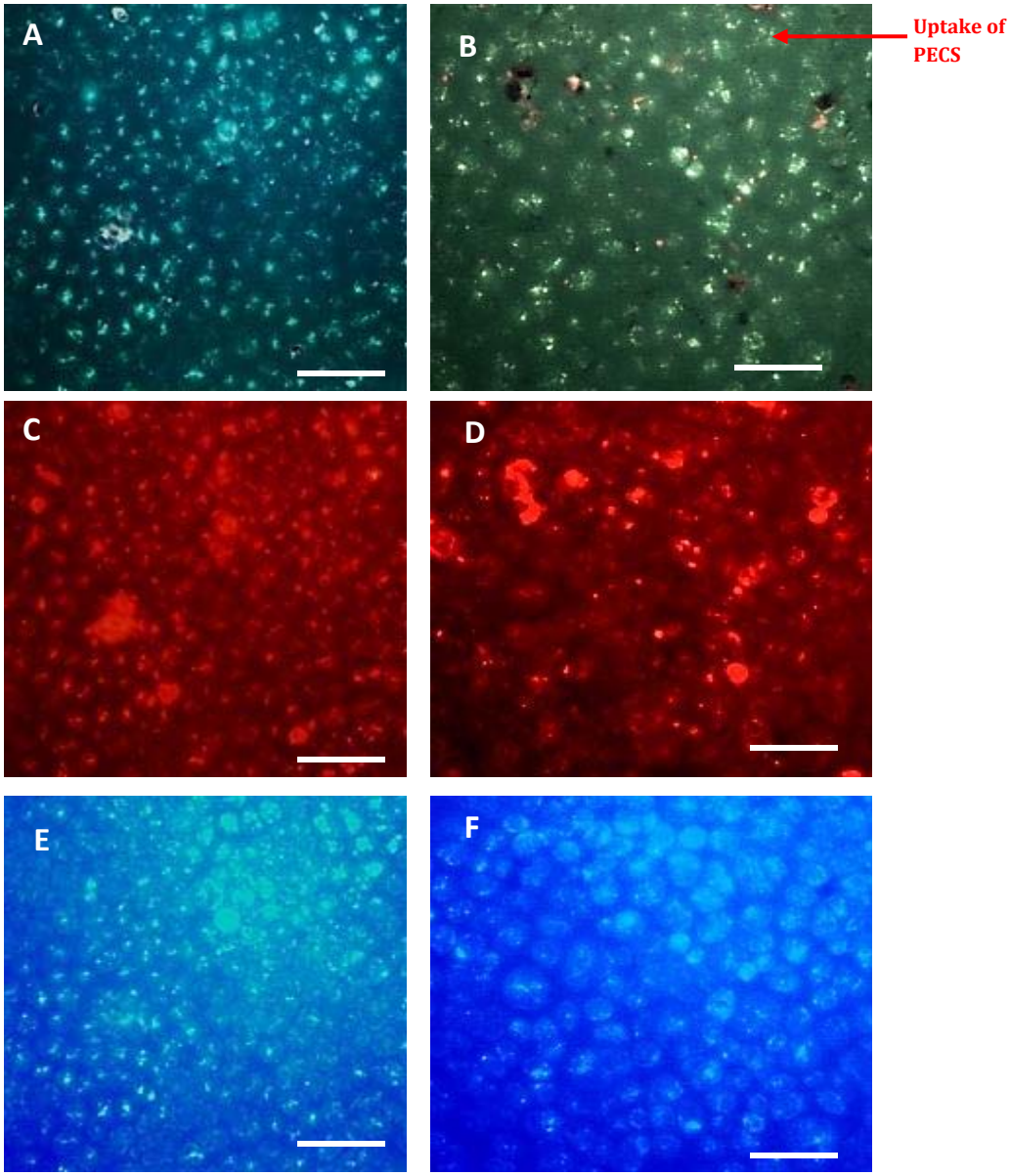

871

872 **Fig. 13**: Fluorescent microscopy images of Caco-2 cells post treatment with QPAA-TBA, insulin complexes in A) normal
873 media-RBITC/FITC combination filter B) calcium-free media-RBITC/FITC combination filter C) normal media-RBITC
874 filter D) calcium free media-RBITC filter E) normal media-FITC filter F) calcium free media-FITC filter. Scale bar-50
875 µm.

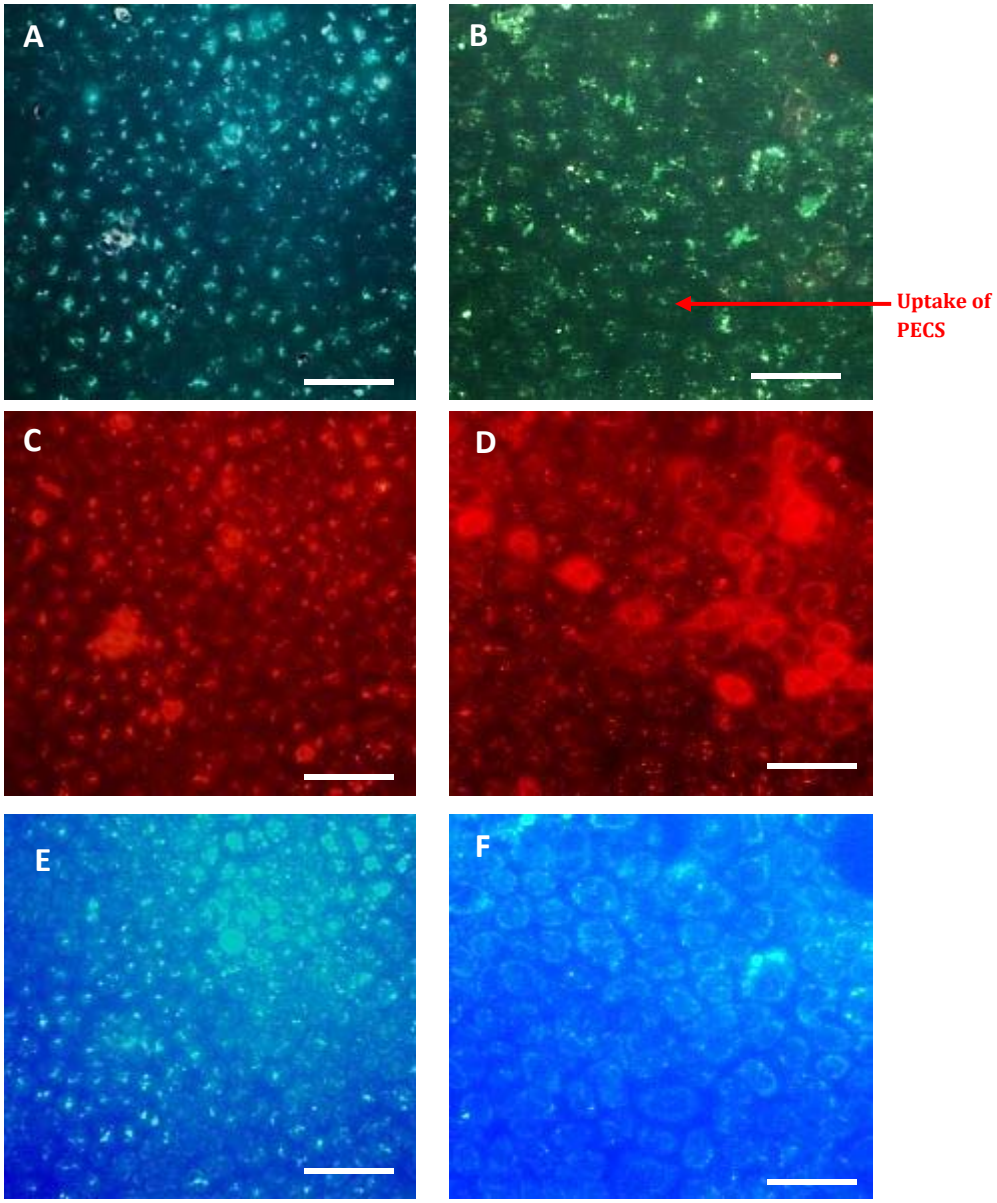

876

877 **Fig. 14**: Fluorescent microscopy images of Caco-2 cells treated with QPAA-TBA, insulin complexes where cell insulin

878 receptors are A) normal-RBITC/FITC combination filter B) pre-saturated with insulin-RBITC/FITC combination filter C)

879 normal-RBITC filter D) pre-saturated with insulin-RBITC combination filter E) normal-FITC filter F) pre-saturated with

880 insulin-FITC combination filter. Scale bar-50 µm.

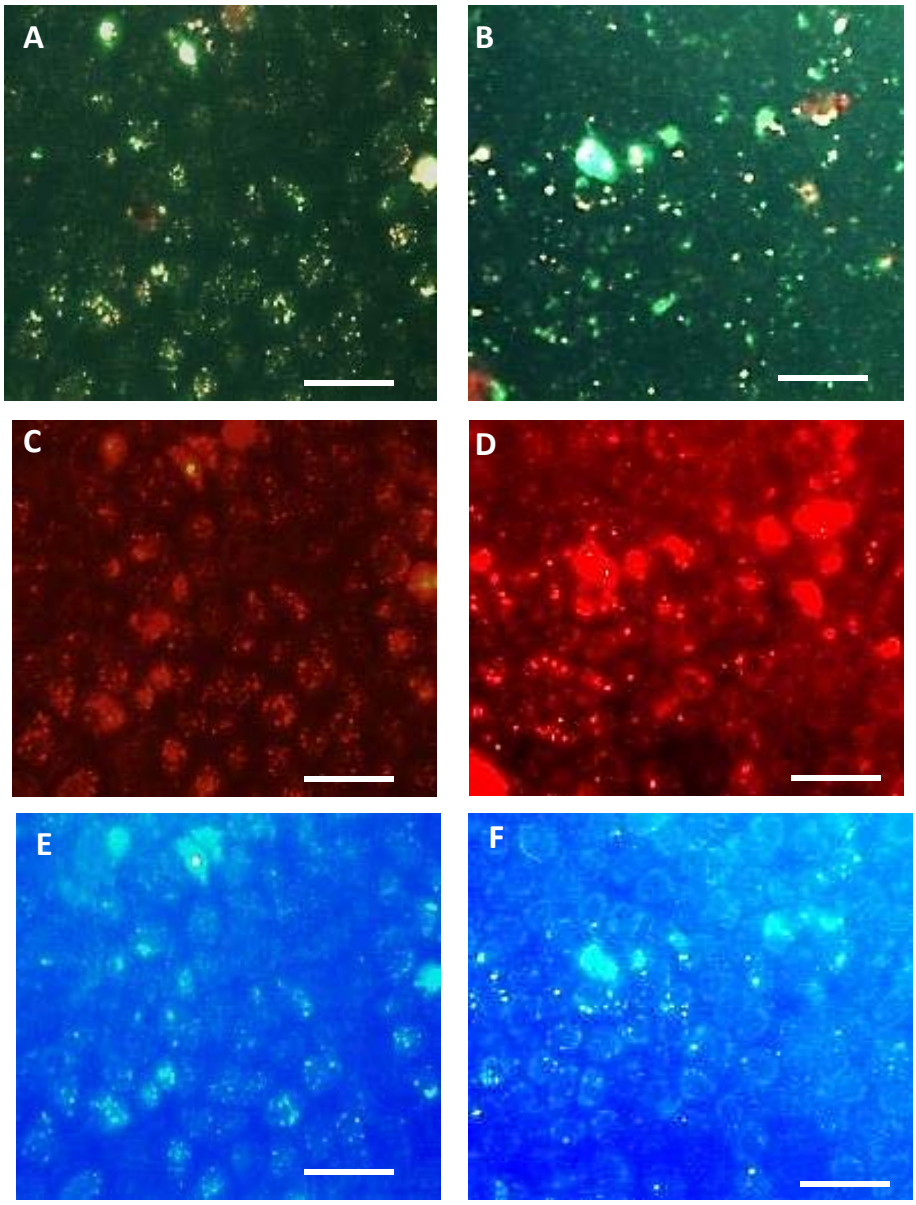

881

882 **Fig. 15**: Fluorescent microscopy images of Caco-2 cells treated with QPAA, insulin complexes where cell insulin receptors
883 are A) normal-RBITC/FITC combination filter B) pre-saturated with insulin-RBITC/FITC combination filter C) normal-
884 RBITC filter D) pre-saturated with insulin-RBITC combination filter E) normal-FITC filter F) pre-saturated with insulin-
885 FITC combination filter. Scale bar-50 µm.

886

887

888

889

890

Table 1: Free thiol content, disulphide bond content, total thiol content and zeta potential of polymers. Values are mean ± S.D. (n = 3).

Polymer	Free thiol content ($\mu mol g^{-1}$)	S-S bond content ($\mu mol g^{-1}$)	Total thiol substitution ($\mu mol g^{-1}$)	Zeta Potential (mV)
PAA	n/a	n/a	n/a	41.9 ± 2
QPAA	n/a	n/a	n/a	45.0 ± 3
PAA-NAC	60 ± 1.2	280	340 ± 4.1	35.7 ± 1
QPAA-NAC	60 ± 4.3	220	280 ± 3.3	37.4 ± 1
PAA-TBA	490 ± 18	590	1080 ± 28	46.9 ± 1
QPAA-TBA	440 ± 21	560	1000 ± 31	48.4 ± 1

Table 2: IC_{50} values ($mgml^{-1}$) of PAA, QPAA and thiolated derivatives obtained without/with a 24 h recovery period. Values are mean ± S.D. (n = 3).

	PAA	**QPAA**	**PAA-NAC**	**QPAA-NAC**	**PAA-TBA**	**QPAA-TBA**
Without Recovery Period	0.009 ± 0.003	0.062 ± 0.001	0.011 ± 0.009	0.036 ± 0.003	0.023 ± 0.002	0.024 ± 0.003
With Recovery Period	0.013 ± 0.005	>4	0.064 ± 0.002	0.144 ± 0.007	0.033 ± 0.009	0.110 ± 0.003

Table 3: Concentration of polymer at which a significant ($p<0.05$) drop of cell viability is observed when compared to the respective vehicle control.

	Paa	**QPaa**	**Paa-NAC**	**QPaa-NAC**	**Paa-TBA**	**QPaa-TBA**
Without Recovery Period	0.02	0.08	0.02	0.08	0.03	0.05
With Recovery Period	0.03	NA	0.1	0.1	0.03	1.0

Table 4: Level of significant difference in cell viability with vehicle control for each of the polymers at each of the concentrations tested (n=3).

Polymer concentration (mg/ml)	PAA		PAA-NAC		PAA-TBA		QPAA		QPAA-NAC		QPAA-TBA	
	Without Recovery Period	With Recovery Period	Without Recovery Period	With Recovery Period	Without Recovery Period	With Recovery Period	Without Recovery Period	With Recovery Period	Without Recovery Period	With Recovery Period	Without Recovery Period	With Recovery Period
1	NS	NS	NS	NS	NS	NS	NS	NS	NS	NS	NS	NS
5	NS	NS	NS	NS	NS	NS	NS	NS	NS	NS	NS	NS
8	NS	NS	NS	NS	NS	NS	NS	NS	NS	NS	NS	NS
10	NS	NS	NS	NS	NS	NS	NS	NS	NS	NS	NS	NS
20	***	NS	*	NS	NS	NS	NS	NS	NS	NS	NS	NS
30	***	*	***	NS	**	NS	NS	NS	NS	NS	NS	NS
40	***	***	***	NS	**	*	NS	NS	NS	NS	NS	NS
50	***	***	***	NS	*	*	NS	NS	NS	NS	**	NS
80	***	***	***	NS	***	**	NS	NS	*	NS	*	NS
100	***	***	***	**	***	***	*	NS	*	*	**	NS
1000	***	***	***	***	***	***	***	NS	***	**	***	***

Key: NR = NO RECOVERY PERIOD; R = RECOVERY PERIOD; NS = NOT SIGNIFICANT I.E. P>0.05; *= P<0.05; ** = P<0.01; *** = P<0.001.

Table 5: Percentage uptake of incubated polymer mass by Caco-2 cells. Values are mean ± S.D. (n=3).

	PAA	QPAA	QPAA-NAC	QPAA-TBA
% Polymer uptake	12.55 ± 0.83	22.88 ± 1.77	26.48 ± 1.40	28.50 ± 0.38

925

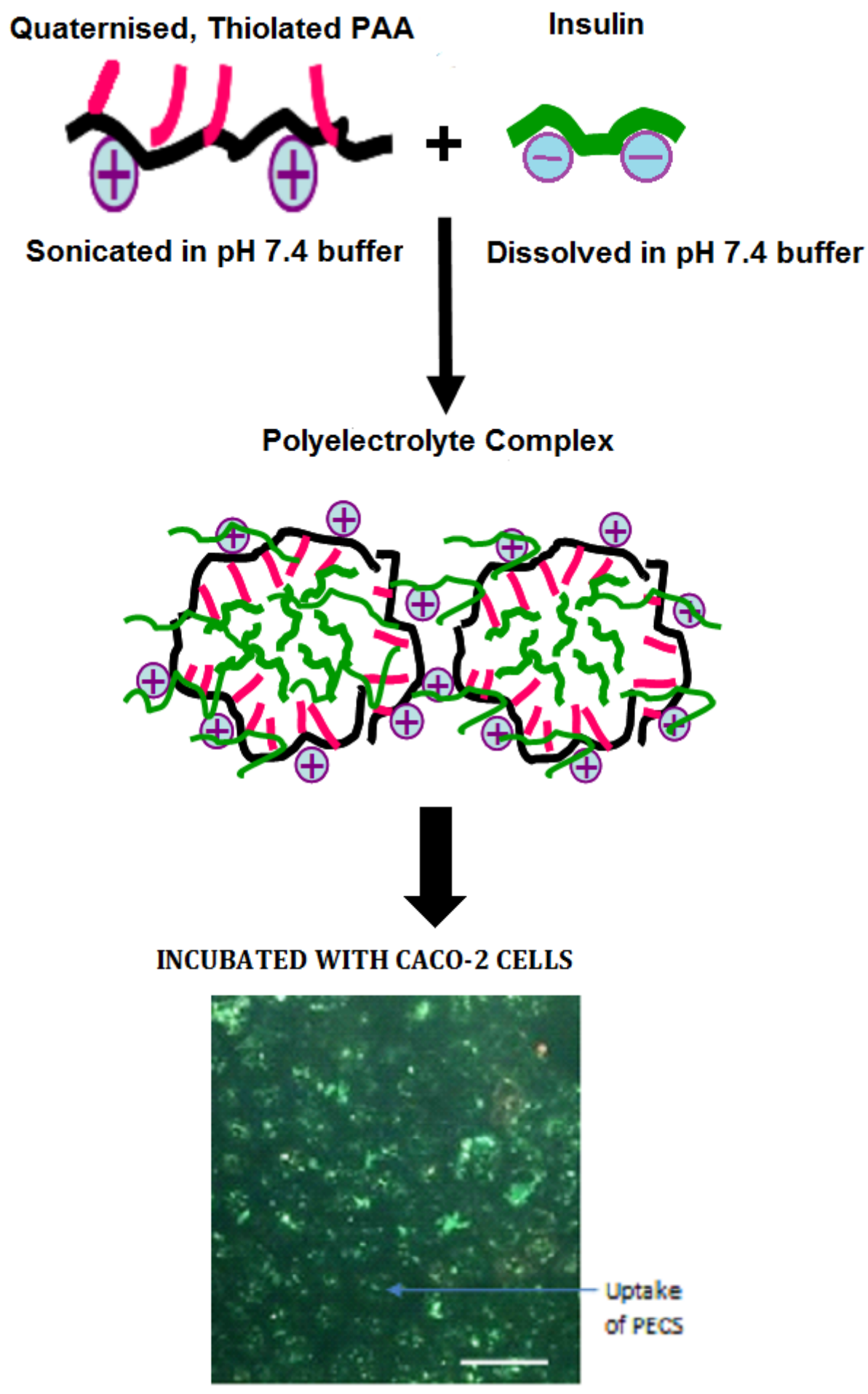
Quaternised, Thiolated PAA
Insulin
Sonicated in pH 7.4 buffer
Dissolved in pH 7.4 buffer
Polyelectrolyte Complex
INCUBATED WITH CACO-2 CELLS
Uptake
of PECS

926

927